IN SEARCH OF HIDDEN SECTOR THROUGH THE MONO-PHOTON CHANNEL

A THESIS SUBMITTED TO
THE GRADUATE SCHOOL OF NATURAL AND APPLIED SCIENCES
OF
MIDDLE EAST TECHNICAL UNIVERSITY

BY

ENFAL SARTAŞ

IN PARTIAL FULFILLMENT OF THE REQUIREMENTS
FOR
THE DEGREE OF MASTER OF SCIENCE
IN
PHYSICS

DECEMBER 2022

Approval of the thesis:

IN SEARCH OF HIDDEN SECTOR THROUGH THE MONO-PHOTON CHANNEL

submitted by **ENFAL SARTAŞ** in partial fulfillment of the requirements for the degree of **Master of Science in Physics Department, Middle East Technical University** by,

Prof. Dr. Halil Kalıpçılar
Dean, Graduate School of **Natural and Applied Sciences** _____

Prof. Dr. Seçkin Kürkcüoğlu
Head of Department, **Physics** _____

Prof. Dr. İsmail Turan
Supervisor, **Physics, METU** _____

Examining Committee Members:

Prof. Dr. İsmet Yurduşen
Mathematics, Hacettepe University _____

Prof. Dr. İsmail Turan
Physics, METU _____

Assoc. Prof. Dr. Levent Selbuz
Physics Engineering, Ankara University _____

Date: 02.12.2022

I hereby declare that all information in this document has been obtained and presented in accordance with academic rules and ethical conduct. I also declare that, as required by these rules and conduct, I have fully cited and referenced all material and results that are not original to this work.

Name, Surname: Enfal Sartaş

Signature :

ABSTRACT

IN SEARCH OF HIDDEN SECTOR THROUGH THE MONO-PHOTON CHANNEL

Sartaş, Enfal
M.S., Department of Physics
Supervisor: Prof. Dr. İsmail Turan

December 2022, 71 pages

A growing body of experimental and observational evidence shows that Standard Model calculations account for only 5% of the mass and energy of the universe. The remainder consists of dark matter and dark energy, which have yet to be observed. This indicates that what has been revealed so far is only the tip of the iceberg. The existence of dark matter, first discovered by Fritz Zwicky, suggests the presence of a hidden sector that is almost neutral under any of the forces predicted by the Standard Model. Within the framework of the portal concept, the vector portal, which brings its own additional dark gauge symmetry, is one of the proposed portals connecting the hidden sector with the Standard Model sector. Holding an additional gauge symmetry also means having an extra gauge field, hence a gauge boson. The traces of this gauge boson, namely the dark photon, are intended to be separated from the SM background in the context of this thesis.

Research on the mono-photon channel is carried out within the framework of a $B-L$ model, which is established to explore the decay and production processes of a light-dark photon (in the order of MeV-GeV), and corresponding results are obtained. First, the Lagrangian of the $B-L$ model is created with the assistance of the FeynRules

program, and therefore the model's mass matrices and interaction vertices are obtained through this program. Then, a model interface is constructed employing the FeynRules program once more for the Madgraph package program that will be used to examine the production and decay channels.

In addition to neutrinos, one of the possible undercover decay channels of the dark photon is the decay channel to a dark matter pair. Therefore, the missing energy ($\not{E}$) in the signal of the mono-photon channel ($\gamma + \not{E}$) needs to contain not only SM particles but also dark matter particles, depending on the model structure. At the final stage of the analysis, the interaction between dark matter and SM particles via the dark photon is also taken into account.

Keywords: physics beyond the standard model, hidden sector, dark sector, dark matter, vector portal, mono-photon channel

ÖZ

TEK-FOTON KANALI ÜZERİNDEN SAKLI SEKTÖR ARAYIŞINDA

Sartaş, Enfal
Yüksek Lisans, Fizik Bölümü
Tez Yöneticisi: Prof. Dr. İsmail Turan

Aralık 2022 , 71 sayfa

Artan sayıda deneysel ve gözlemsel kanıt, Standart Model hesaplamalarının evrenin kütlesinin ve enerjisinin yalnızca %5'ini oluşturduğunu göstermektedir. Geri kalan ise, henüz gözlemlenmemiş olan karanlık madde ve karanlık enerjiden oluşmaktadır. Bu durum, şu ana kadar ortaya çıkanların buzdağının sadece görünen kısmı olduğu anlamına gelmektedir. İlk olarak Fritz Zwicky tarafından keşfedilen karanlık maddenin varlığı, Standart Model tarafından tahmin edilen kuvvetlerin herhangi biri altında neredeyse nötr olan gizli bir sektörün varlığını akla getirmektedir. Portal konsepti çerçevesinde, kendi ek karanlık ayar simetrisine sahip olan vektör portalı, gizli sektörü Standart Model sektörüyle birleştirmek için önerilen portallardan bir tanesidir. Ek ayar simetrisine sahip olmak, aynı zamanda fazladan bir ayar alanına, dolayısıyla bir ayar bozonuna sahip olmak anlamına gelmektedir. Bu tez kapsamında, bu ayar bozonunun yani karanlık fotonun izlerinin SM arka planından ayrıştırılması amaçlanmıştır.

Tek-foton kanalı ile ilgili çalışmalar, hafif bir karanlık fotonun (MeV-GeV mertebesinde) bozunum ve üretim süreçlerini araştırmak için kurulan bir $B - L$ modeli

çerçevesinde yürütülmüş ve buna karşılık gelen sonuçlar elde edilmiştir. Öncelikle FeynRules programı yardımıyla $B - L$ modelinin Lagranjiyeni oluşturulmuş ve bu nedenle modelin kütle matrisleri ve etkileşim köşeleri bu program aracılığıyla elde edilmiştir. Daha sonra üretim ve bozunum kanallarının incelenmesinde kullanılacak olan Madgraph paket programı için yine FeynRules programı kullanılarak bir model arayüzü oluşturulmuştur.

Nötrinolara ek olarak, karanlık fotonun olası gizli bozunum kanallarından biri de karanlık madde çiftine giden bozunum kanalıdır. Bu nedenle, model yapısına bağlı olarak, tek-foton kanalının ($\gamma + \not{E}$) sinyalindeki kayıp enerjinin ($\not{E}$) yalnızca SM parçacıklarını değil, aynı zamanda karanlık madde parçacıklarını da içermesi gerekir. Analizin son aşamasında SM parçacıkları ile karanlık madde arasında karanlık foton aracılığıyla var olan etkileşim de dikkate alınmıştır.

Anahtar Kelimeler: standart model ötesi fizik, saklı sektör, karanlık sektör, karanlık madde, vektör portal, tek-foton kanalı

Abim Cem Sandal'a...

"In visions of the dark night
I have dreamed of joy departed
But a waking dream of life and light
Hath left me broken-hearted..."

ACKNOWLEDGMENTS

First and foremost, I would like to convey my heartfelt gratitude to my thesis advisor, Prof. Dr. İsmail Turan, for making his extensive knowledge available to me and for his guidance through the entire process. Furthermore, I would like to thank him for treating me like a brother when necessary, sharing his life experiences, most importantly, understanding me when I needed to be understood. I do not think this work would have been possible without his support and advice.

I would like to thank Prof. Dr. Takhmasib M. Aliyev for the insightful discussions we shared, for his encouragement, and for always being a guiding light for me. I would also like to thank Assoc. Prof. Dr. Levent Selbuz for his support and guiding attitude.

It is not enough to thank Prof. Dr. Şinasi Ellialtıoğlu for our sweet conversations, for allowing me to create my own workspace and develop myself, and for taking care of me without restricting my freedom in that workspace, and also for being an excellent supervisor. I hope to have the opportunity to work with him for many more years.

I would like to express my special thanks to Ahmet Azgın for his deep friendship, for taking on the role of a savior, and for being with me on both bright and dark days. I would also like to thank Giray Mecit, Esra Akyumuk, and Alaittin Kırtışoğlu for their priceless efforts during the completion of this work.

I cannot pass up the chance to thank my entire family for standing beside me, especially my brother Furkan and my sister Büşra, as well as Seviha and Barbaros, who are just like siblings to me.

More than anyone and anything, I am eternally grateful to my loving, caring, and supportive wife, Feriha Sartaş, for turning my life into an enjoyable experience, for making me feel valuable all the time, for her endless sacrifices, for her gaze, her smile, her love, and for not depriving me of these.

TABLE OF CONTENTS

ABSTRACT v

ÖZ vii

ACKNOWLEDGMENTS x

TABLE OF CONTENTS xi

LIST OF TABLES xiv

LIST OF FIGURES xv

LIST OF ABBREVIATIONS xvii

CHAPTERS

1 INTRODUCTION 1

2 STANDARD MODEL 3

2.1 Interactions of the SM 4

2.1.1 $U(1)$ Gauge Invariance and Quantum Electrodynamics 4

2.1.2 $SU(2)_L \otimes U(1)_Y$ Electroweak Interaction 6

2.1.3 $SU(3)$ Strong Interaction 11

2.1.4 SSB and Mass Acquisition Mechanism for Gauge Bosons . . . 13

2.2 Problems of the SM and Motivation for the BSM Studies 16

2.2.1 Number of Free Parameters 17

2.2.2 Grand Unification 18

2.2.3 Higgs Mass Fine Tuning . . . 19
2.2.4 Strong CP Problem . . . 19
2.2.5 Neutrino Oscillations . . . 19
2.2.6 Baryon Asymmetry . . . 20
2.2.7 Anomalous Magnetic Dipole Moment of the Muon . . . 20
2.2.8 Dark Energy . . . 20
2.3 Dark Matter . . . 21
2.3.1 Relic Density . . . 21
2.3.2 Weakly Interacting Massive Particles (WIMPS) . . . 23
2.3.3 Axions . . . 23
2.3.4 Sterile Neutrinos . . . 24
2.3.5 Asymmetric Dark Matter (ADM) . . . 24
3 HIDDEN SECTOR . . . 25
3.1 Scalar Portal . . . 26
3.2 Neutrino Portal . . . 27
3.3 Vector Portal . . . 28
4 THE SM AND HIDDEN SECTOR WITH ABELIAN GAUGE GROUP . . . 29
5 COMPACT LINEAR COLLIDER . . . 35
5.1 New Physics Searches at CLIC . . . 37
6 NUMERICAL ANALYSIS . . . 39
6.1 Some Kinematical Variables . . . 39
6.2 Madgraph Simulation Results . . . 40
6.2.1 DP Only Case . . . 40

6.2.2 DP + DM Case 45

6.2.2.1 Relic Density Computation 48

7 CONCLUSION 49

REFERENCES 51

APPENDICES

Appendices 57

A FEYNMAN DIAGRAMS 59

A.1 Feynman Diagrams at SM Level 59

A.2 Feynman Diagrams with Hidden Sector Contribution (DP Only) . . . 61

A.3 Feynman Diagrams with Hidden Sector Contribution (DM Involved) . 70

LIST OF TABLES

TABLES

Table 2.1 Parameters of the Electroweak Part 7

Table 2.2 Parameters of the Standard Model 18

Table 5.1 Parameters of the CLIC energy stages. 36

Table 6.1 Cross-section values of contributions from SM and dark photon (DP) to the mono-photon + missing energy signal ($e^-e^+ \rightarrow \gamma\nu_l\bar{\nu}_l$) at CLIC energy levels. The dark sector parameters are selected as $M'_A = 10$ GeV, $g_{B-L} = 0.1$ and $sin\epsilon = 10^{-4}$. 41

Table 6.2 Studied Parameters for the CLIC - Stage 3 (3 TeV) 43

Table 6.3 Cross-section values of contributions from DP and DP + DM processes to the mono-photon + missing energy signal ($e^-e^+ \rightarrow \gamma\nu_l\bar{\nu}_l$) at CLIC energy levels. The dark sector parameters are selected given in the Table 6.4. 45

Table 6.4 Studied Parameters for DP + DM Case 45

LIST OF FIGURES

FIGURES

Figure 2.1 Fundamental gluon vertices 13

Figure 5.1 The footprint of a future CLIC accelerator with energy stages of 380 GeV, 1.5 TeV and 3 TeV (Image credit: CERN) 35

Figure 6.1 Distribution of events according to some variables by using Pythia and Delphes at 380 GeV center of mass energy for the ($e^-e^+ \rightarrow \gamma\nu_l\bar{\nu}_l$) process in CLIC. ($e^-$,$e^+$) beam polarizations are taken as (-80%, -30%). 41

Figure 6.2 Distribution of events according to some variables by using Pythia and Delphes at 1500 GeV center of mass energy for the ($e^-e^+ \rightarrow \gamma\nu_l\bar{\nu}_l$) process in CLIC. ($e^-$,$e^+$) beam polarizations are taken as (-80%, -30%). 42

Figure 6.3 Distribution of events according to some variables by using Pythia and Delphes at 3000 GeV center of mass energy for the ($e^-e^+ \rightarrow \gamma\nu_l\bar{\nu}_l$) process in CLIC. ($e^-$,$e^+$) beam polarizations are taken as (-80%, -30%). 44

Figure 6.4 Distribution of events according to some variables by using Pythia and Delphes at 380 GeV center of mass energy for the ($e^-e^+ \rightarrow \gamma\chi\bar{\chi}$) process in CLIC. ($e^-$,$e^+$) beam polarizations are taken as (-80%, -30%). 46

Figure 6.5 Distribution of events according to some variables by using Pythia and Delphes at 3000 GeV center of mass energy for the ($e^-e^+ \rightarrow \gamma\chi\bar{\chi}$) process in CLIC. ($e^-$,$e^+$) beam polarizations are taken as (-80%, -30%). 47

Figure A.1 1st set of diagrams of the process: $e^-e^+ > \gamma\nu_\mu\bar{\nu}_\mu$ 59

Figure A.2 1st set of diagrams of the process: $e^-e^+ > \gamma\nu_e\bar{\nu}_e$ 60

Figure A.3 1st set of diagrams of the process: $e^-e^+ > \gamma\nu_e\bar{\nu}_e$ 61

Figure A.4 2nd set of diagrams of the process: $e^-e^+ > \gamma\nu_e\bar{\nu}_e$ 62

Figure A.5 3rd set of diagrams of the process: $e^-e^+ > \gamma\nu_e\bar{\nu}_e$ 63

Figure A.6 4th set of diagrams of the process: $e^-e^+ > \gamma\nu_e\bar{\nu}_e$ 63

Figure A.7 1st set of diagrams of the process: $e^-e^+ > \gamma\nu_\mu\bar{\nu}_\mu$ 64

Figure A.8 2nd set of diagrams of the process: $e^-e^+ > \gamma\nu_\mu\bar{\nu}_\mu$ 65

Figure A.9 3rd set of diagrams of the process: $e^-e^+ > \gamma\nu_\mu\bar{\nu}_\mu$ 66

Figure A.10 1st set of diagrams of the process: $e^-e^+ > \gamma\nu_\tau\bar{\nu}_\tau$ 67

Figure A.11 2nd set of diagrams of the process: $e^-e^+ > \gamma\nu_\tau\bar{\nu}_\tau$ 68

Figure A.12 3rd set of diagrams of the process: $e^-e^+ > \gamma\nu_\tau\bar{\nu}_\tau$ 69

Figure A.13 1st set of diagrams of the process: $e^-e^+ > \gamma\chi\bar{\chi}$ 70

Figure A.14 2nd set of diagrams of the process: $e^-e^+ > \gamma\chi\bar{\chi}$ 71

LIST OF ABBREVIATIONS

SM	Standard Model
QED	Quantum Electrodynamics
QCD	Quantum Chromodynamics
SU(N)	Special Unitary Group with Degree of N
SBS	Symmetry Breaking Sector
SSB	Spontaneous Symmetry Breaking
WS	Weinberg-Salam
SLAC	Stanford Linear Accelerator Center
vev	vacuum expecatition value
em	electromagnetism
CKM	Cabibbo–Kobayashi–Maskawa
C	Charge conjugation
CP	Charge conjugation-Parity
CPT	Charge conjugation-Parity-Time reversal
EW	Electroweak
CMB	Cosmic Microwave Background
DM	Dark Matter
HDM	Hot Dark Matter
CDM	Cold Dark Matter
WIMP	Weakly Interacting Massive Particle
GUT	Grand Unified Theory
MSM	Minimal Standard Model
ADM	Asymmetric Dark Matter
HS	Hidden Sector

LHC	Large Hadron Collider
int	interaction
HNL	Heavy Neutral Lepton
KE	Kinetic Energy
KM	Kinetic Mixing
CLIC	Compact Linear Collider
HL-LHC	High Luminosity Large Hadron Collider
IP	interaction point
LINAC	Linear Accelerator
BSM	Beyond the Standard Model
DP	Dark Photon

CHAPTER 1

INTRODUCTION

The Standard Model (SM) is the most accurate model we have right now for describing the fundamental particles that are the universe's building blocks, how they interact with each other, and their interaction mechanisms [1]. Thanks to technological improvements, experiments conducted up to this point have shown that the Standard Model is accurate. Nevertheless, there are some basic questions that the Standard Model is insufficient to explain or cannot answer at all, which is why it should only be seen as an effective model [2]. This incompleteness raises the possibility that the Standard Model is a low-energy version of a more fundamental theory. The physics existing in the region between the energy scale of the Standard Model and that of this possible fundamental theory is called new physics. One of the most substantial pieces of evidence for new physics is the existence of dark matter, which does not interact with the known fundamental forces other than gravity, has not yet been discovered and indicates the existence of a hidden sector (also known as the dark sector).

The universe has been attempted to be correctly understood above the electroweak energy scale, either by extending the Standard Model gauge group, adding new groups, or considering it with larger gauge groups combined instead. One would anticipate having a single set of gauge groups with representations for the high-scale energies required by unified theories. As these anticipated gauge groups break, additional groups may remain alongside the G_{SM} group while descending to the electroweak scale. It is also necessary for there to be new gauge bosons if there are going to be any extra gauge groups. Since the W and Z bosons were discovered in the 1980s [3, 4], physicists have been looking into the indirect effects of gauge bosons on sensitive electroweak tests and trying to track these bosons in colliders. Unfortunately,

there has not been any discovery of such gauge bosons up to this point. This situation has led the physics realm to think that new gauge bosons are heavy and have much higher energies than the electroweak scale [5, 6]. This sector might have a complicated gauge structure with scalar, fermionic, and vector fields [7, 8, 9]. In this thesis, the main focus is on the vector field case and the extension of SM via the vector portal.

In order to investigate the existence of a hidden sector containing new particles beyond the SM in accelerator experiments, namely in linear colliders, a vector portal model was created. Although these accelerators are not designed to detect low-mass particles, it seems possible to investigate hidden sector traces in these accelerators utilizing the mono-photon signal [10]. One factor that makes this possible is that the SM background of the mono-photon signal is low. Assuming SM fermions have quantum charges under the hidden sector gauge group, the dark photon and SM fermions can interact proportional to the coupling constant, g_D. In the framework of the model adopted in this thesis, the dark photon can interact with all SM particles with a $B-L$ number other than zero, where B is the baryon number, whereas L is the lepton number. This study focuses on the phenomenology of the hidden light sector. An examination of the production and decay channels of a light-mass dark photon (MeV to GeV) within the $B-L$ model is carried out. FeynRules is used to generate the Lagrangian of the model, mass matrices, and interaction terms. Besides, the model's interface for the Madgraph package program is also produced with the help of FeynRules. In this context, the Compact Linear Collider, a low-energy, high-luminosity electron-positron collider, is being considered in the analysis [11]. Such colliders are ideal for the search for new light particles because they have significant production rates and high-precision resonance reconstruction capabilities [12].

CHAPTER 2

STANDARD MODEL

The Standard Model is a renormalizable quantum field theory that describes the behavior of the fundamental matter [13]. An essential feature of this model is that both the electroweak and the strong force are introduced as gauge interactions [14]. In this description, three separate parts can be defined:

1. The matter sector consists of the fermion field

2. The vector boson gauge field

3. The symmetry breaking sector (SBS)

The SBS, which is needed for massive fermions and electroweak bosons, is not as well established as the other two sectors [14]. Since 1947, particle physicists have known of a consistent layer of reality that exists on its own, unaffected by the external world. This layer of reality has been revealed to be the basis of all physical reality. The SM requires lots of free parameters, but it does not explain these parameters; they may be evidence for a deeper understanding of the nature of reality [15]. Despite the fact that processes described by the Standard Model are incredibly insensitive to signals from new physics, the model appears to be a good enough approximation to describe all existing data. This theoretical structure has been successful up to this point, and it is thought that the new physics will simply be an extension of the standard model rather than an invalidator of it.

2.1 Interactions of the SM

Both particles that carry "charge" and particles that "mediate" interactions between currents by coupling directly to charge are considered to be constituents of a gauge theory. The fundamental fermions and non-abelian gauge bosons are members of the first class, while the second class is made up entirely of gauge bosons, which can either be abelian or non-abelian. Depending on the particular theory, a charge might have different physical properties. The Standard Model predicts three of these charge types: color, weak isospin, and weak hypercharge. These charges must be calculated empirically for each particle because their values cannot be anticipated by gauge symmetry. The strength of the interaction between a gauge boson and a particle depends on the particle's charge. For instance, the electron-photon coupling constant is denoted by $-e$, but the strength of the interaction between a u-quark and a photon is denoted by $2e/3$. Non-abelian gauge bosons interact with themselves since they are both charge carriers and mediators. These result in significant nonlinearities, which make it difficult to solve non-abelian gauge theories mathematically. In general, particle masses are not determined by gauge symmetry. Even though the concept of gauge symmetry would seem to conflict with gauge-boson mass, the Weinberg-Salam model includes a dynamical method, the Higgs mechanism, for producing mass for both gauge bosons and fermions [16].

2.1.1 $U(1)$ Gauge Invariance and Quantum Electrodynamics

Throughout the course of history, electrodynamics was the earliest of the gauge field theories. Its updated form, known as Quantum Electrodynamics (QED), is now the physics theory that has been the most completely tested since its construction. The Standard Model both incorporates and expands QED, making it the greatest possible way to start learning about the model.

Considering the transformation:

$$\psi(x) \rightarrow e^{i\alpha(x)}\psi(x) \tag{2.1}$$

where $\alpha(x)$ varies in an entirely arbitrary fashion depending on both space and time. This phenomenon is referred to as "local gauge invariance." Nevertheless, this does

not produce the desired results. The Lagrangian,

$$\mathcal{L} = \bar{\psi}(i\gamma^{\mu}\partial_{\mu} - m)\psi \tag{2.2}$$

does not preserve its invariance under these kinds of local phase transformations. By using (2.1) one can write,

$$\bar{\psi} \rightarrow e^{-i\alpha(x)}\bar{\psi} \tag{2.3}$$

Therefore, the second component of $\mathcal{L}$ is invariant; yet, the derivative of the field breaks the invariance due to the last term of the expression below.

$$\partial_{\mu}\psi \rightarrow e^{i\alpha(x)}\partial_{\mu}\psi + ie^{i\alpha(x)}\psi\partial_{\mu}\alpha \tag{2.4}$$

In order to make the Lagrangian invariant under the local gauge transformations, we need to look for a covariant derivative that provides us with the invariance under phase transformations.

$$D_{\mu}\psi \rightarrow e^{i\alpha(x)}D_{\mu}\psi \tag{2.5}$$

where e is the electric charge for ψ. The covariant derivative, D_{μ}, can be constructed by introducing a vector field, A_{μ} as

$$D_{\mu} \equiv \partial_{\mu} - ieA_{\mu} \tag{2.6}$$

whereas the new vector field transforms as

$$A_{\mu} \rightarrow A_{\mu} + \frac{1}{e}\partial_{\mu}\alpha \tag{2.7}$$

By replacing ∂_{μ} with the covariant derivative, D_{μ}, (2.2) can be modified as

$$\mathcal{L} = i\bar{\psi}\gamma^{\mu}D_{\mu}\psi - m\bar{\psi}\psi = \bar{\psi}(i\gamma^{\mu}\partial_{\mu} - m)\psi + e\bar{\psi}\gamma^{\mu}A_{\mu}\psi \tag{2.8}$$

Hence, since we insist on maintaining phase invariance at the local level, we are compelled to formulate a vector field named the gauge field. This field couples to the Dirac particle in the very same manner that the photon field does. The new interaction term can be denoted as $j^{\mu}A_{\mu}$, where j^{μ} refers to the current density.

A kinetic energy term must be included in the Lagrangian to consider this vector field as the physical photon field. For the sake of gauge invariance, the kinetic term, it is only possible for the field strength tensor to be involved.

$$F_{\mu\nu} = \partial_{\mu}A_{\nu} - \partial_{\nu}A_{\mu} \tag{2.9}$$

At the end, the Lagrangian can be written as

$$\mathcal{L} = -\frac{1}{4}F_{\mu\nu}F^{\mu\nu} + \bar{\psi}(i\gamma^{\mu}\partial_{\mu} - m)\psi + e\bar{\psi}\gamma^{\mu}A_{\mu}\psi \tag{2.10}$$

Note that the inclusion of the mass term cannot take place since gauge invariance precludes it. The photon, which serves as a gauge particle, must be massless. As a result, it is reasonable to anticipate that the gauge field will have an unlimited range [15].

2.1.2 $SU(2)_L \otimes U(1)_Y$ Electroweak Interaction

Like its predecessor QED, the electroweak theory, i.e. the Glashow-Weinberg-Salam model [17, 18, 19], is a gauge theory meaning that interactions are derived from symmetries. It possesses the group structure $SU(2)_L \otimes U(1)_Y$, where $SU(2)_L$ and $U(1)_Y$ respectively stand for weak isospin and weak hypercharge. Only left-handed states of fermions undergo nontrivial transformations when weak isospin is introduced, as indicated by the letter 'L' in the $SU(2)_L$. Since the extension to the SM will be through the electroweak section in this study, this section will be discussed in detail.

To begin, we will go over assigning the quantum numbers for the fermionic weak isospin and the weak hypercharge. We assume that each succeeding generation of fermions differs from the one that came before it simply in terms of their mass. As a result, it is unnecessary to consider anything other than the lightest fermions for the sake of simplicity. Table 2.1 shows the electroweak assignments for the first generation fermions.

Table 2.1: Parameters of the Electroweak Part

$SU(2) \otimes U(1)$ assignments			
Particle	T	T_3	Y
$v_{e,L}$	$1/2$	$1/2$	-1
e_L	$1/2$	$-1/2$	-1
$v_{e,R}$	0	0	0
e_R	0	0	-2
u_L	$1/2$	$1/2$	$1/3$
d_L	$1/2$	$-1/2$	$1/3$
u_R	0	0	$4/3$
d_R	0	0	$-2/3$

The left-handed doublets of the leptons can be introduced at this point:

$$L_e = \begin{pmatrix} \nu_e \\ e^- \end{pmatrix}_L \quad , \quad L_\mu = \begin{pmatrix} \nu_\mu \\ \mu^- \end{pmatrix}_L \quad \text{, and} \quad L_\tau = \begin{pmatrix} \nu_\tau \\ \tau^- \end{pmatrix}_L \tag{2.11}$$

$$R_{e,\mu,\tau} = e_R, \mu_R, \tau_R \tag{2.12}$$

In contrast to the left-handed leptons, right-handed ones are isospin singlets ($I = 0$). Through the well-known Gell-Mann–Nishijima formula, $Q = T_3 + \frac{Y}{2}$, the weak hypercharges are choosen to possess the observed electric charges.

By using the same notation, the hadronic sector can also be represented as

$$L_q^{(1)} = \begin{pmatrix} u \\ d \end{pmatrix}_L \quad , \quad L_q^{(2)} = \begin{pmatrix} c \\ s \end{pmatrix}_L \quad \text{, and} \quad L_q^{(3)} = \begin{pmatrix} t \\ b \end{pmatrix}_L \tag{2.13}$$

while their right-handed correspondents are

$$R_u^i = u_R, c_R, t_R \quad \text{, and} \quad R_d^i = d_R, s_R, b_R \tag{2.14}$$

where i runs from 1 to 3. The right-handed quarks are isospin singlets as their counterparts in the leptonic sector. Considering that we need $\mathcal{L}$ to be invariant under local rotations of the doublet, we impose $SU(2)$ gauge invariance solely on the left-handed

doublets. Therefore, different charges of elements of the doublet are ignored. Likewise, their distinct masses are ignored in the Yukawa mass matrix. Only left-handed states are subject to the gauge symmetry, resulting in an entirely left-right antisymmetric weak interaction [20].

After the quantum numbers have been allocated, we will move on to the electroweak interactions. The Weinberg–Salam Lagrangian naturally splits up into three different parts that add together:

$$\mathcal{L}_{WS} = \mathcal{L}_G + \mathcal{L}_F + \mathcal{L}_H \tag{2.15}$$

where the subscripts G, F, and H, represent gauge, fermion, and Higgs, respectively. Indeed there should be a mass term for the fermions in the Lagrangian in the form of

$$\mathcal{L}_{\text{mass}} = -m\bar{\psi}\psi = -m(\bar{\psi}_L\psi_R + \bar{\psi}_R\psi_L) \tag{2.16}$$

However, since the left-handed fermions are doublet as the right-handed ones are singlet under $SU(2)$, the Lagrangian would not be invariant under a gauge transformation due to the mass term.

The gauge fields,$\vec{W}_\mu = (W^1_\mu, W^2_\mu, W^3_\mu)$ and B_μ, coupling to the weak isospin and hypercharge contribute solely to the gauge part of the Lagrangian as

$$L_G = -\frac{1}{4}F^{\mu\nu}_i F^i_{\mu\nu} - \frac{1}{4}B^{\mu\nu}B_{\mu\nu} \tag{2.17}$$

where $F^i_{\mu\nu}$ and $B_{\mu\nu}$ are the field strengths of $SU(2)$ and $U(1)$ respectively.

$$F^i_{\mu\nu} = \partial_\mu W^i_\nu - \partial_\nu W^i_\mu - g\epsilon^{ijk}W^j_\mu W^k_\nu \tag{2.18}$$

$$B_{\mu\nu} = \partial_\mu B_\nu - \partial_\nu B_\mu \tag{2.19}$$

On the other hand, the fermionic sector Lagrangian consists of both left and right-handed chiralities and can be written as

$$\mathcal{L}_F = \sum_{\psi_L} \bar{\psi}_L i\not{D}\psi_L + \sum_{\psi_R} \bar{\psi}_R i\not{D}\psi_R \tag{2.20}$$

Since the right-handed fermions are singlets and do not couple to the weak isospin, the covariant derivative applies to them is

$$D_\mu\psi_R = (\partial_\mu - i\frac{g'}{2}YB_\mu)\psi_R \tag{2.21}$$

while its counterpart for the left-handed fermions takes the form

$$D_\mu \psi_L = (\partial_\mu - i\frac{g'}{2} Y B_\mu - i\frac{g}{2}\vec{\tau}.\vec{W}_\mu)\psi_L \tag{2.22}$$

Hence, an interaction term appears in the Lagrangian:

$$\mathcal{L}_{\text{free}} \rightarrow \mathcal{L}_{\text{free}} - g\vec{W}_\mu.\vec{J}^{\mu}_{\text{weak}} \tag{2.23}$$

where the weak current is

$$\vec{J}^{\mu}_{\text{weak}} = \bar{\psi}_L \gamma^\mu \vec{T} \psi_L \tag{2.24}$$

Gauge fields, $W^{(1)}$, $W^{(2)}$ and $W^{(3)}$ couple to the left-handed doublets. In order to make them interact with currents of the physical leptons, they should be recast into the fields of physical gauge bosons, $W^{\pm}$ and Z^0 [21].

$SU(2)$ generators, the well-known Pauli spin matrices, can be shown as

$$\tau_1 = \begin{pmatrix} 0 & 1 \\ 1 & 0 \end{pmatrix} \quad , \quad \tau_2 = \begin{pmatrix} 0 & -i \\ i & 0 \end{pmatrix} \quad \text{and} \quad \tau_3 = \begin{pmatrix} 1 & 0 \\ 0 & -1 \end{pmatrix} \tag{2.25}$$

where the first two of them mix with components of a doublet while the last one does not.

$$\begin{aligned} \vec{T}.\vec{W}_\mu &= \frac{1}{2}(\tau_1 W^{(1)}_\mu + \tau_2 W^{(2)}_\mu + \tau_3 W^{(3)}_\mu) \\ &= \frac{1}{2}\begin{pmatrix} W^{(1)}_\mu & W^{(1)}_\mu - iW^{(2)}_\mu \\ W^{(1)}_\mu + iW^{(2)}_\mu & -W^{(3)}_\mu \end{pmatrix} \end{aligned} \tag{2.26}$$

and the fields are defined as

$$W^{\pm}_\mu = \frac{1}{\sqrt{2}}(W^{(1)}_\mu \mp iW^{(2)}_\mu) \tag{2.27}$$

In equation 2.27 index $\pm$ refers to the electric charge. However, we have not shown that these fields are electrically charged yet. In order to show that the coupling between W fields and charge lowering/raising currents should be investigated. Starting with the definition of charged current in terms of the interaction Lagrangian,

$$\mathcal{L}_{\text{charged}} = -g(W^{(1)}_\mu J^{1\mu} + W^{(2)}_\mu J^{2\mu}) \tag{2.28}$$

where

$$J^{1\mu} = \bar{\psi}_L \gamma^\mu \frac{\tau_1}{2} \psi_L \qquad \text{and} \qquad J^{2\mu} = \bar{\psi}_L \gamma^\mu \frac{\tau_2}{2} \psi_L \tag{2.29}$$

so that the Lagrangian can be rewritten as

$$\mathcal{L}_{\text{charged}} = -g(W_\mu^+ J^{+\mu} - W_\mu^- J^{-\mu}) \tag{2.30}$$

with

$$J^{\pm\mu} = \frac{1}{\sqrt{2}} \bar{\psi}_L \gamma^\mu \tau^\pm \psi_L \tag{2.31}$$

where $\tau^\pm = \frac{1}{2}(\tau_1 \pm i\tau_2)$. Ultimately, the leptonic charge raising and lowering currents can be written respectively as

$$J^{+\mu} = \frac{1}{2\sqrt{2}} \bar{\nu}\gamma^\mu(1-\gamma^5)e \qquad \text{and} \qquad J^{-\mu} = \frac{1}{2\sqrt{2}} \bar{e}\gamma^\mu(1-\gamma^5)\nu \tag{2.32}$$

Interactions involving neutral current results from the third component of the weak isospin field

$$\mathcal{L}_{\text{int}} = -gW_\mu^3 J_3^\mu \tag{2.33}$$

where the conserved current is given as

$$J_3^\mu = \bar{\psi}_L \gamma^\mu \frac{\tau_3}{2} \psi_L \tag{2.34}$$

We must continue with a different $U(1)$ gauge symmetry known as "weak hypercharge". We demand that it commutes with the $SU(2)_L$ generators and denote its generator with Y. The individual members of the isospin multiplet then acquire the same hypercharge value by construction. The combined symmetry is represented by $SU(2)_L \otimes U(1)_Y$. In light of this, a left-handed doublet becomes

$$\psi_L \to e^{i(\vec{\alpha}(x)\vec{T} + \beta(x)Y)} \psi_L \tag{2.35}$$

where Y is the generator for $U(1)_Y$ and $T = \tau/2$ are the $SU(2)$ generators we used previously. By the time, right-handed components transform only under weak hypercharge as

$$\psi_R \to e^{i\beta(x)Y} \psi_R \tag{2.36}$$

so the conserverd current associated with $U(1)_Y$ is

$$J_Y^\mu = \bar{\psi}\gamma^\mu Y \psi \tag{2.37}$$

Eventually, the interaction can be denoted in closed form as

$$\mathcal{L}_{\text{EW}} = \sum_\psi \bar{\psi}\gamma^\mu(\partial_\mu - i\frac{g'}{2} Y B_\mu - ig\vec{T}.\vec{W}_\mu)\psi \tag{2.38}$$

and together with equation 2.17 defines the complete electroweak Lagrangian. In order to accomplish the Weinberg-Salam Lagrangian, we will discuss the spontaneous symmetry breaking and Higgs mechanism in Section 2.1.4. In this way, we will allow $W^{\pm}$ and Z^0 to acquire their physical masses that we cannot provide at this point for the sake of gauge invariance.

2.1.3 $SU(3)$ Strong Interaction

The theory known as quantum chromodynamics (QCD), which describes the strong force that exists between quarks and gluons, is constructed in a manner that is quite similar. Evidence for quarks was found for the first time in electron-proton scattering events that took place at SLAC.

One can start by considering the free Lagrangian

$$\mathcal{L}_0 = \bar{q_j}(i\gamma^\mu \partial_\mu - m)q_j \tag{2.39}$$

for a color triplet,

$$q = \begin{pmatrix} q_r \\ q_g \\ q_b \end{pmatrix} \quad \text{and} \quad \bar{q} = \begin{pmatrix} \bar{q_r} & \bar{q_g} & \bar{q_b} \end{pmatrix} \tag{2.40}$$

Following the same techniques outlined in section 2.1.1 allows us to provide local gauge invariance on the Lagrangian, 2.39. Simply taking into account following infinitesimal phase transformations

$$\begin{aligned} q(x) &\rightarrow Uq(x) \equiv e^{i\alpha_a(x)T_a}q(x) \\ \partial_\mu q &\rightarrow (1 + i\alpha_a T_a)\partial_\mu q + iT_a q \partial_\mu \alpha_a \end{aligned} \tag{2.41}$$

where $T_a = \frac{\lambda_a}{2}$ are the required Gell-Mann matrices that are the generators of the gauge field for $SU(3)$ with $a = 1, 2, ..., 8$ and α_a are the real group parameters. Since the commutation relation $[T_a, T_b]$ is not satisfied for all the generators, the group is called non-abelian. Indeed,

$$[T_a, T_b] = if_{abc}T_c \tag{2.42}$$

is the commutation relation for these matrices. Here, f_{abc} is the structure constant. One can easily show that the structure constant is totally anti-symmetric by multiplying both sides of 2.42 by another group member and taking the trace.

However the last term in 2.41 breaks down the invariance of the Lagrangian. It is possible for us to proceed in the same manner with QED and to bring in gauge fields, denoted by G_μ^a, transforming as

$$G_\mu^a \to G_\mu^a - \frac{1}{g_s}\partial_\mu \alpha_a \tag{2.43}$$

and construct the covariant derivative

$$D_\mu = \partial_\mu + i g_s T_a G_\mu^a \tag{2.44}$$

so that we the Lagrangian can be written as

$$\mathcal{L} = \bar{q}(i\gamma^\mu \partial_\mu - m)q - g_s(\bar{q}\gamma^\mu T_a q)G_\mu^a \tag{2.45}$$

Unlike the $U(1)$ case, this is not enough to generate a gauge invariant Lagrangian. We can rewrite the gauge fields, G_μ^a as

$$G_\mu^a \to G_\mu^a - \frac{1}{g_s}\partial_\mu \alpha_a - f_{abc}\alpha_b G_\mu^c \tag{2.46}$$

Nevertheless, none of those mentioned above expressions adequately describe the QCD theory by itself. In order to complete the $SU(3)$ gauge invariance, it is necessary to identify the strength tensor for the kinetic term.

$$G_{\mu\nu}^a = \partial_\mu G_\nu^a - \partial_\nu G_\mu^a - g_s f_{abc} G_\mu^b G_\nu^c \tag{2.47}$$

To provide the gauge invariance, the last term in the strength tensor here defines the self-interaction of gluon fields shown in Figure 2.1 and makes it quite different from its counterpart in QED, in which photons are not allowed to interact with each other. Finally, QCD Lagrangian can be finalized as

$$\mathcal{L} = -\frac{1}{4}G_{\mu\nu}^a G_a^{\mu\nu} + \bar{q}(i\gamma^\mu \partial_\mu - m)q - g_s(\bar{q}\gamma^\mu T_a q)G_\mu^a \tag{2.48}$$

In opposition to the abelian case, non-abelian gauge theories include an explicit component proportional to the coupling constant within the gauge transformation. Such that fermions coupling to gauge fields feel the same amount of strength regardless of the distance within the interaction range (as long as the flux tube is unbroken). Otherwise, there would be inconsistencies in theory. As a direct result of the non-abelian character, the running coupling constant at high energies becomes small while it is significant at low energies [22]. This phenomenon is called asymptotic freedom.

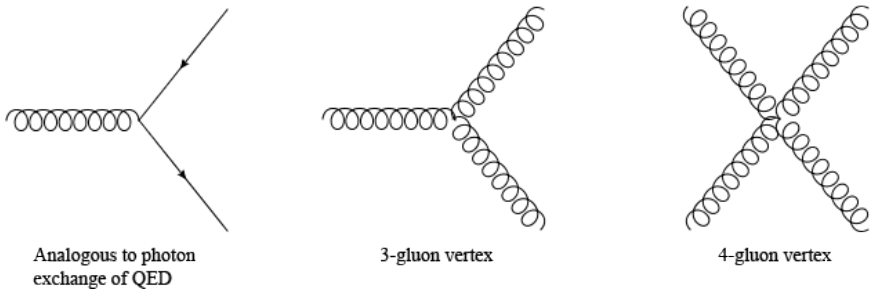


Figure 2.1: Fundamental gluon vertices

QCD may be characterized at short distances in terms of weakly interacting quarks and gluons, whereas the theory becomes non-perturbative at longer distances to provide the quark confinement. Consequently, we can only detect color-singlet bound states of three quarks, three antiquarks, or quark-antiquarks pairs. This implies that quarks cannot be observed as free states [23].

2.1.4 SSB and Mass Acquisition Mechanism for Gauge Bosons

The concept of spontaneous symmetry breaking will be applied to the $SU(2)_L \otimes U(1)_Y$ gauge symmetry in this section. It will be demonstrated that by choosing specific parameters in a particular way, it is possible to obtain massive Z and W bosons while maintaining the masslessness of the photon. In order to achieve this, one can introduce a complex isospin doublet with weak isospin $\frac{1}{2}$:

$$\phi = \begin{pmatrix} \phi^+ \\ \phi^0 \end{pmatrix} = \frac{1}{\sqrt{2}} \begin{pmatrix} \phi_1 + i\phi_2 \\ \phi_3 + i\phi_4 \end{pmatrix} \tag{2.49}$$

where the superscripts represent electric charges of the components of the left-handed doublet to ensure the hypercharge to be $Y = 1$. After, the potential that will break the symmetry spontaneously can be defined

$$V(\phi) = \mu^2(\phi^\dagger\phi) + \lambda(\phi^\dagger\phi)^2 \quad \text{, with} \quad \mu^2 < 0 \tag{2.50}$$

At first look, the addition of a $V(\phi)$ term to the Lagrangian in the form of equation 2.50 might be thought of as adding a particle with imaginary mass ($\mu^2 < 0$). However, when we look at the particle spectrum using the perturbations around the vacuum, we find that it genuinely depicts a massive scalar particle (one with a real and

positive mass) with three and four-point self-interactions. Besides, λ must be positive in order to guarantee the absolute minimum of the Lagrangian. Even though the Lagrangian maintains its initial symmetry (symmetry in ϕ), the vacuum does not exhibit symmetry in the newly introduced field; this phenomenon is known as spontaneous symmetry breaking. Please note that we have given the theory one additional degree of freedom in the form of a scalar particle so that the part added to the Lagrangian is

$$\mathcal{L}_{\text{scalar}} = (D^{\mu}\phi)^{\dagger}(D_{\mu}\phi) - V(\phi) \tag{2.51}$$

however, this Lagrangian is not gauge invariant by itself. It is essential to remember that the inclusion of $\mathcal{L}_{\text{gauge}}$ is mandatory to save the invariance. And the equation for the covariant derivative

$$D_{\mu} = \partial_{\mu} + i\frac{g}{2}\vec{\tau}.\vec{W}_{\mu} + i\frac{g'}{2}YB_{\mu} \tag{2.52}$$

Choosing the vacuum expectation value (vev) so that the positive component of the doublet would be absent in the ground state in agreement with reality, as

$$\langle\phi_0\rangle = \frac{1}{\sqrt{2}}\begin{pmatrix}0\\v\end{pmatrix} \tag{2.53}$$

This choice is also appropriate for $U(1)_{em}$ gauge invariance and will lead us to the massless photon. As a result, the SSB mechanism describes how the gauge bosons' polarization vector receives the Goldstone bosons' degrees of freedom.

One can check the invariance of the symmetries in the given vacuum state by using the generators as:

- For $SU(2)_L$

$$\tau_1\phi_0 = \begin{pmatrix}0 & 1\\1 & 0\end{pmatrix}\frac{1}{\sqrt{2}}\begin{pmatrix}0\\v\end{pmatrix} = \frac{1}{\sqrt{2}}\begin{pmatrix}v\\0\end{pmatrix} \neq 0$$

$$\tau_2\phi_0 = \begin{pmatrix}0 & -i\\i & 0\end{pmatrix}\frac{1}{\sqrt{2}}\begin{pmatrix}0\\v\end{pmatrix} = -\frac{i}{\sqrt{2}}\begin{pmatrix}v\\0\end{pmatrix} \neq 0$$

$$\tau_3\phi_0 = \begin{pmatrix}1 & 0\\0 & -1\end{pmatrix}\frac{1}{\sqrt{2}}\begin{pmatrix}0\\v\end{pmatrix} = -\frac{1}{\sqrt{2}}\begin{pmatrix}0\\v\end{pmatrix} \neq 0$$

- For $U(1)_Y$

$$Y\phi_0 = Y_{\phi_0}\frac{1}{\sqrt{2}}\begin{pmatrix}0\\v\end{pmatrix} = \frac{1}{\sqrt{2}}\begin{pmatrix}0\\v\end{pmatrix} \neq 0$$

These broken symmetries imply that the vacuum state stays neutral because the ground state does not follow the initial $SU(2)_L \otimes U(1)_Y$ symmetry of the Lagrangian but rather belongs to the sub-symmetric group $U(1)_{em}$. This behavior is the fundamental concept behind a smaller gauge symmetry choice by a larger symmetry group after the symmetry breaking.

- For $U(1)_{em}$

$$Q\phi_0 = \frac{1}{2}(\tau_3 + Y)\phi_0 = \begin{pmatrix}1 & 0\\0 & 0\end{pmatrix}\frac{1}{\sqrt{2}}\begin{pmatrix}0\\v\end{pmatrix} = 0$$

In order to obtain masses of the gauge bosons, a small perturbation should be applied to the complex scalar doublet around the vev. It is necessary to identify a parametrization of the scalar doublet around ϕ_0 to accurately describe the excitations that originate from the vacuum.

$$\phi(x) = \frac{1}{\sqrt{2}}\begin{pmatrix}0\\v + h(x)\end{pmatrix} \tag{2.54}$$

where $H(x) = v + h(x)$ is the field responsible from Higgs boson whose vev is v, $\langle H_0(x)\rangle = v$.

In order to give rise to masses of the gauge bosons, one can start employing the covariant derivative given in equation 2.52 and write down the quadratic terms in matrix form by choosing the eigenvalue of weak hypercharge as $Y = 1$

$$\mathcal{L}_{\text{mass}} = \frac{1}{8}\begin{pmatrix}0 & v\end{pmatrix}\begin{pmatrix}gW_\mu^{(3)} + g'B_\mu & g(W_\mu^{(1)} - iW_\mu^{(2)})\\ g(W_\mu^{(1)} + iW_\mu^{(2)}) & -gW_\mu^{(3)} + g'B_\mu\end{pmatrix}^2\begin{pmatrix}0\\v\end{pmatrix} \tag{2.55}$$

Weinberg angles are defined in order to diagonalize the mass-squared matrix.

$$\theta_w = \arctan(g'/g) \tag{2.56}$$

so the fields are

$$W_\mu^{\pm} = \frac{1}{\sqrt{2}}(W_\mu^{(1)} \mp iW_\mu^{(2)}) \tag{2.57}$$

$$Z_\mu = W_\mu^{(3)} \cos\theta_w - B_\mu \sin\theta_w \tag{2.58}$$

$$A_\mu = W_\mu^{(3)} \sin\theta_w + B_\mu \cos\theta_w \tag{2.59}$$

In terms of fields, equation 2.55 becomes

$$\mathcal{L}_{\text{mass}} = (gv/2)^2 W^{+\mu} W_\mu^- + \frac{1}{2}(gv/\cos\theta_w) Z^\mu Z_\mu \tag{2.60}$$

and this leads to

$$M_W = gv/2 \tag{2.61}$$

$$M_Z = M_W/\cos\theta_w \tag{2.62}$$

Notice that the photon field remains massless because of the smaller symmetry choice mentioned earlier. For more detailed calculation, one can see [24, 25, 26].

2.2 Problems of the SM and Motivation for the BSM Studies

The SM created a prescription for combining forces via spontaneous symmetry breaking and gauge symmetry. As expansions of the SM, the grand unified theories, supergravity, and string theories were established. We anticipate the existence of a new physics outside the standard model, just as the theories of relativity and quantum mechanics emerged as a consequence of studies beyond classical mechanics and electromagnetism. Fortunately, the development of unified theories enabled us to better understand the early universe's history. The SM also implemented the idea that the discovery of a new particle equates to the discovery of a new physics [27].

However, we are confident that the Standard Model of particle physics does not represent the final word. The finding of neutrino oscillations is one convincing piece of evidence. It highlights that the SM assumptions are inaccurate because at least two out of three SM neutrinos are massive. Rubin's and Ford's finding of dark matter based on rotation curve measurements is another piece of evidence. It implies that the SM cannot explain a sizable percentage of the universe's material.

Along with the above-mentioned issues, the SM falls short of many theorists' expectations. The gauge symmetries have not yet been united by the model, and it is still unable to explain why particles are governed by $SU(3) \otimes SU(2) \otimes U(1)$ structure.

Today, rather than seeing the Standard Model as a fundamental explanation of nature up to the Planck scale, we see it as an effective theory. Some SM problems will be briefly discussed in this section; however, a more in-depth examination of dark matter will be covered in the subsequent section.

2.2.1 Number of Free Parameters

There are 13 parameters in the Yukawa interactions, including the masses of three charged leptons and six quarks, in addition to three CKM angles and the CP-violating phase. The challenge to this sector is the problem of flavor. Besides, four parameters make up the gauge sector of the SM, including the gauge couplings and an additional CP-violating phase this time in QCD. The challenge of simplifying this sector is the matter of unification. Finally, the quartic and quadratic couplings are the two parameters of the minimal Higgs sector. The issue with this sector is nothing but the problem of mass. The SM has a total number of 19 free parameters in total. Considering this many free parameters, believing that the SM is the end of the story is not that easy.

Table 2.2: Parameters of the Standard Model

Parameters of the Standard Model	
Symbol	**Value**
m_e	511 keV
m_μ	105.7 MeV
m_τ	1.78 GeV
m_u	1.9 GeV
m_d	4.4 MeV
m_s	87 MeV
m_c	1.32 GeV
m_b	4.24 GeV
m_t	172.7 GeV
θ_{12}	13.1°
θ_{23}	2.4°
θ_{13}	0.2°
δ	0.995
g'	0.357
g	0.652
g_s	1.221
θ_{QCD}	~ 0
v	246 GeV
m_H	125.36 ± 0.41 GeV

2.2.2 Grand Unification

Three of the fundamental forces are described by the SM. During this description, electromagnetic and weak forces can be combined to be represented by the electroweak force, while the strong force is left untouched. The strong force is strong, as the others are weak at low energy; however, because of the behavior of running cou-

pling constants as the energy increases, they all would tend to get together in terms of strength. Therefore it is a natural thought that maybe they all come together at some point, and we may have the grand unification we have been looking for [28, 29].

2.2.3 Higgs Mass Fine Tuning

The standard model of particle physics includes a single scalar field, known as the Higgs field, which is responsible for the mass of other particles in the model. However, it is not clear how the mass of the Higgs field itself can be protected against quantum corrections that would otherwise cause it to increase significantly without the use of extremely precise adjustments. Several different solutions have been proposed to address this problem, including the incorporation of low-scale supersymmetry [30], the inclusion of additional spatial dimensions [31], and the use of dynamic relaxation mechanisms [32]. These approaches offer potential ways to stabilize the mass of the Higgs field and avoid the need for fine-tuning.

2.2.4 Strong CP Problem

It is possible for there to be a violation of the CP symmetry in strong interactions, according to the mathematical model of QCD that is currently in use. However, in every experiment containing just the strong interaction, there has never been any evidence of a violation of the CP symmetry [33]. Since there is no justification for CP symmetry to be preserved in strong interactions, this problem is referred to as the strong CP problem.

2.2.5 Neutrino Oscillations

Experimentally observed neutrino oscillations indicate that at least two of three neutrinos are massive [34, 35], which is not present in the SM. The fact that the measured neutrino masses are so much less than the masses of other leptons presents another problem for the explanation. The "see-saw mechanism", which introduces at least one heavy sterile neutrino, is a typical technique for producing such a mass matrix

[36]. When this heavy mass scale is added to the SM scales, it makes it possible for the EW neutrinos to have very light mass eigenstates.

2.2.6 Baryon Asymmetry

An equal quantity of matter and antimatter should have been created when the Big Bang formed the universe. However, all of the structure we can observe now is made of matter, and there is no evidence to suggest that large quantities of antimatter exist. There must have been some event that tipped the balance. Out of equilibrium phenomena in the early universe that violated baryon number conservation together with the C and CP symmetries may be used to explain the imbalance between matter and antimatter. When symmetric initial conditions and CPT conservation are assumed, the generation of the baryon asymmetry requires the fulfillment of the Sakharov conditions [37]. In order to put these conditions into effect, the SM needs to be extended in some fashion [38].

2.2.7 Anomalous Magnetic Dipole Moment of the Muon

The anomalous magnetic dipole moment of the muon is a measure of the deviation of the muon's magnetic moment from the value that it would have if it were purely magnetic [39]. It is an important quantity in particle physics because it provides a way to test the Standard Model. Furthermore, it is related to the behavior of virtual particles, which can contribute to the deviation from the expected value of the muon's magnetic moment. The most precise measurement of the magnetic dipole moment of the muon was made by the Muon g-2 experiment at Fermilab, and the result is in good agreement with the prediction of SM [40]. However, the measurement also leaves room for the possibility of new physics beyond the Standard Model.

2.2.8 Dark Energy

CMB observations reveal that our universe underwent an exponential expansion phase at the beginning and is presently going through a second accelerated phase [41]. None

of these phases of the universe's development are explained by the SM. The widely accepted explanation for these observations is that the remaining 70% of the universe is made up of dark energy, which is thought to penetrate space and accelerate the expansion of the universe.

Other phenomena such as the possible lepton universality violation in B-meson decays [42] and the anomalous mass of the W boson [43] have also been reported recently.

2.3 Dark Matter

Fritz Zwicky initially proposed the possibility of dark matter in 1933 to explain the strange motion of galaxies in the Coma Cluster [44]. However, it was long forgotten until observations of the rotational motion of spiral galaxies made with the aid of the 21-cm bright hydrogen lines brought it back to life in the 1970s [45]. Today, it is known that many galaxy clusters contain dark matter. Some evidence [46, 47] for the presence of dark matter can be given as,

- Rotational curves of spiral galaxies
- Virial mass of the clusters
- X-ray emitting clusters
- Gravitational lensing

while a set of classification is provided by analysis of the structural formation:

- Hot Dark Matter (HDM): Relativistic at the time of freeze-out
- Cold Dark Matter (CDM): Nonrelativistic at the time of freeze-out

2.3.1 Relic Density

The relic density of DM is a measure of the abundance of DM particles in the present-day universe, expressed as a fraction of the total number of particles. It is an essential

quantity in the study of DM, as it can provide insight into the nature and properties of DM particles.

In the early universe, DM particles were in thermal equilibrium with ordinary matter, meaning they were constantly created and destroyed through interactions with other particles. The rate at which these interactions occurred as determined by the universe's temperature, which was much higher in the early universe due to the high energy density of the hot, dense plasma of particles that filled the universe.

As the universe cooled and expanded, the DM particle interaction rate slowed. At a certain point, known as the "freeze-out" temperature, the rate of DM particle interactions became too slow to maintain thermal equilibrium. This occurred when the universe's expansion began dominating the interactions between DM and ordinary matter. At this point, the number density of DM particles stopped increasing and began to decrease due to the universe's expansion [27].

The present-day relic density of DM is determined by the number of DM particles that survived the freeze-out process. This can be expressed as [48]:

$$\Omega_{\text{DM}} = (n_{\text{DM}}/n_{\text{tot},0}) \tag{2.63}$$

where Ω_{DM} is the present-day relic density of DM, $(n_{\text{DM}}/n_{\text{tot},0})$ is the present-day ratio of the number density of DM particles (n_{DM}) to the total number density of particles $(n_{\text{tot},0})$, and the subscript "0" indicates the present-day value.

The exact value of the relic density depends on the properties of the DM particles, such as their mass and their interactions with ordinary matter. These properties can be described using a set of parameters known as the "freeze-out parameters." The freeze-out parameters can be used to calculate the present-day relic density by employing a set of equations known as the "Boltzmann equations," which describe the DM particle number density evolution over time.

There are several ways to measure the relic density of DM, including observations of CMB radiation, gravitational lensing, and the distribution of matter in galaxies. In recent years, the most precise measurements of the relic density have come from the Planck satellite, which observed the cosmic microwave background radiation across the entire sky [46, 47].

2.3.2 Weakly Interacting Massive Particles (WIMPS)

The term "Weakly Interacting Massive Particle" (WIMP) refers to a candidate for the DM that is well-motivated theoretically and has a mass in the range of a few GeV to a few TeV. WIMPs typically interact with particles described by the SM through the Electroweak sector, and they offer the DM abundance that nearly matches the quantity of DM that has been experimentally observed to exist today.

Even if the DM is not a WIMP, a thermal origin is intriguing: DMs of any mass ranging from MeV to TeV scale can acquire the necessary relic abundance by directly annihilating into SM matter [49]. Thermal DM in this range formed as a result of SM interactions excessively in the early universe; hence, plausible scenarios require extra SM neutral mediators to drain the overabundance [50]. Besides, the DM mediators in the sub-GeV range may resolve some outstanding cosmological mysteries, like the issue with the smoother-than-anticipated mass distribution at the center of a galaxy [49]. Additionally, supersymmetry is the most popular of the theories that can account for WIMPS because it also has the added benefit of solving the hierarchy problem in grand unified theories (GUTs) and unifying all forces, including gravity.

2.3.3 Axions

Axions are an additional well-motivated DM contender that may simultaneously solve the strong CP problem originating from the Peccei-Quinn symmetry solution [51]. Even though the WIMP has been the preeminent paradigm of DM theories for the past few decades, axions represent an attractive alternative. As a result of their sufficiently low mass, axion DM particles can only be produced through a non-thermal source, such as gravitational or misalignment production mechanisms. They behave like CDM owing to their collective motion. The acceptable mass range has been significantly constrained due to the unfavorable results of terrestrial experiments and astrophysical observations. Given that an axion can couple to two photons, the Primakov effect will produce a photon with the same energy as the axion mass if the axion passes through a strong electromagnetic field [27].

2.3.4 Sterile Neutrinos

Neutrino oscillation experiments have revealed that neutrinos have non-zero yet extremely tiny masses [34, 35]. The see-saw mechanism [52], which predicts the presence of sterile neutrinos, provides a viable explanation for the neutrino's low mass. Under the SM gauge group, sterile neutrinos are singlets and can mix with active neutrinos. Limits on their parameter space are placed by both astronomical observations and ground-based experiments. A candidate for HDM might be a neutrino with a mass of more than 30 eV but less than 1 MeV. In contrast, the possibility of a light neutrino ($m_\nu \lesssim 1$ MeV) has been ruled out by both accelerator experiments and cosmological considerations. However, if neutrinos with masses greater than $m_\nu < \frac{m_Z}{2}$ do exist, they might be considered as CDM [53]. The Neutrino Minimal Standard Model (νMSM) is a viable example that includes sterile neutrinos.

2.3.5 Asymmetric Dark Matter (ADM)

A primordial asymmetry in cosmological dark matter (DM) hinders the total annihilation of the DM particles with their antiparticles, providing the observed relic density. Asymmetric Dark Matter (ADM) is a DM candidate that originates from this mechanism. The current state of the universe is made up of DM particles without their antiparticles if DM is asymmetric. As a result, the existence of stable bound states of DM particles is an intriguing idea that can affect the characteristics of DM significantly for direct and indirect detection and alter its distribution among galaxies. In the case of ADM, the DM particles (but not their antiparticles) are involved in these bound states [54]. Furthermore, the symmetric part of the ADM might be annihilated due to the coupling with an abelian gauge vector boson, the dark photon, in the early universe, leaving traces in the cosmic microwave background (CMB) and the evolution of galaxies [55].

CHAPTER 3

HIDDEN SECTOR

Despite its flaws, the Standard Model is currently the most effective theory in particle physics. However, it is, by its nature, an insufficient theoretical framework. The SM does not provide a satisfactory explanation for several basic physical phenomena seen in nature, including those discussed in Chapter 2. New physics theories that go "Beyond the Standard Model" make up a significant portion of the work that theoretical physicists publish, making these studies an essential element of the field. New approaches extend the Standard Model so that it is both subtle enough to be compatible with the already available experimental data and influential enough to remedy its problems.

The following typical configuration constitutes the primary basis for the hidden sector framework (the so-called portal framework). Let $\mathcal{O}_{\text{SM}}$ refers to an operator built from SM fields, and $\mathcal{O}_{\text{HS}}$ stands as its counterpart built from fields in the hidden sector. A suitable Lagrangian then for describing the hidden sector framework is

$$\mathcal{L} = \mathcal{L}_{\text{SM}} + \mathcal{L}_{\text{HS}} + \sum_{d=i+j} \frac{1}{\Lambda^{d-4}} \mathcal{O}^i_{\text{SM}} \mathcal{O}^j_{\text{HS}} \tag{3.1}$$

where $\mathcal{L}_{\text{SM}}$ and $\mathcal{L}_{\text{HS}}$ represent the standard model and hidden sector Lagrangians respectively and Λ is the cutoff scale presumably within the range of a TeV and above [56]. There are significant limitations on how the mediator may couple to the SM due to the gauge and Lorentz symmetries of the SM [57]. The sum encompasses a wide range of conceivable operators, each with its own unique composition and dimension. However, only three of them are consistent with the EW symmetry-breaking structure of the SM under the assumption that $\mathcal{O}_{\text{HS}}$ is completely SM neutral. Corresponding

lowest dimensional (dim-4) renormalizable portals in the SM are as follows:

$$\mathcal{L} \supset \begin{cases} (\mu\phi' + \lambda\phi'^2)H^\dagger H & , \text{ Scalar Portal} \\ y_n LHN & , \text{ Neutrino Portal} \\ -\frac{\epsilon}{2\cos\theta_W} F'_{\mu\nu} B^{\mu\nu} & , \text{ Vector Portal} \end{cases} \tag{3.2}$$

where ϕ' denotes the scalar singlet that couples to the Higgs doublet, H, through couplings μ and λ; a novel kind of neutral fermion denoted by N couples to the SM left-handed doublets and the Higgs field through a Yukawa coupling, y_n; and $F'_{\mu\nu}$ is the field strength tensor for the dark photon that couples to the hypercharge field, $B^{\mu\nu}$, with the coupling ϵ and the Weinberg angle θ_W [49].

The vector portal has the major emphasis since the monophoton channel is the primary topic of this thesis; therefore, other portals are mentioned merely for the sake of integrity.

3.1 Scalar Portal

The discovery of the Higgs boson at the Large Hadron Collider (LHC) provides strong evidence for the existence of fundamental scalars in the universe [58, 59]. This discovery also prompts the investigation of the so-called scalar or Higgs portal, which couples the hidden sector to the Higgs boson via the bilinear $H^\dagger H$ operator of the SM [60]. It also encourages the hunt for Higgs-like particles as well as additional studies both for exotic production processes and decay modes of the Higgs. The Higgs boson could be able to provide yet another view into light-hidden sectors, which are made up of particles that are neutral under the SM gauge groups. The minimal scalar portal model has one extra singlet field indicated by the letter ϕ' as well as two couplings, μ and λ. Hence, the interaction Lagrangian can be written as

$$\mathcal{L}_{\text{int}} = (\mu\phi' + \lambda\phi'^2)H^\dagger H = (\mu\phi' + \lambda\phi'^2)hv + ... \tag{3.3}$$

where after the electroweak symmetry is broken spontaneously $H = \frac{1}{\sqrt{2}} \begin{pmatrix} 0 \\ v + h \end{pmatrix}$, and only interaction terms involving the Higgs boson are retained. In other words, the presence of a non-zero μ allows the h and ϕ' states to get mixed. Within the limits of

small mixing, it may be expressed as

$$\theta = \frac{\mu v}{m_h^2 - m_{\phi'}^2} \tag{3.4}$$

Hence, the linear coupling of ϕ' to SM particles can be described as $\theta_{\phi'} \times \sum_{\text{SM}} \mathcal{O}_h$

3.2 Neutrino Portal

Due to their redundancy and their weak interaction scales, neutrinos have been presented as a possible candidate for dark matter. However, it appears impossible to meet the relic density for DM with neutrino masses. Even if neutrinos are assumed to be part of the DM in some models, more is required to explain the expected DM abundance than neutrino abundance, which has an upper limit. There are further constraints on neutrino relic density, but these are out of the scope of this study. On the other hand, the seesaw mechanism is capable of expressing one of the logical justifications for neutrino oscillations. When the existence of a right-handed neutrino is permitted, a potential mass term occurs in the Lagrangian. Consequently, mass eigenvalues of the physical system give rise to two mass eigenvalues. The first is an extremely massive particle, whereas the second is a very light neutrino, and the massive neutrino is a candidate for DM.

The neutrino portal extension of the Standard Model is predicated on the possibility that it is closely related to the process responsible for producing neutrino masses. There are one or more dark fermions within the neutrino portal. These particles are sometimes referred to as heavy neutral leptons or HNLs for short. The interaction Lagrangian for this portal can be expressed as follows:

$$\mathcal{L}_{\text{int}} = \sum F_{\alpha I} (\bar{L}_\alpha H) N_I \tag{3.5}$$

The interaction term in this equation is summed over the flavour of lepton doublets, L_α, and the total number of HNLs that are present, N_I. $F_{\alpha I}$ represents the corresponding Yukawa couplings here. The dark sector Lagrangian must include mass terms for HNLs, which can be of either Majorana or Dirac type [61, 62]. It is possible to obtain $\nu_i - N_J$ mixing parametrized by a matrix, U, by setting the Higgs field to its vev and then diagonalizing the mass terms for neutral fermions. Furthermore, ν_α can

be replaced with $\sum_I U_{\alpha I} N_I$ to obtain interactions of HNLs inside the SM interaction terms. The components of the U-matrix are responsible for controlling not only the production but also the decay of HNLs in the minimal HNL models [49].

3.3 Vector Portal

The generation of the vector portal is based on the idea that a dark sector vector boson can couple to the SM gauge bosons through kinetic mixing. This mixing can be induced in a one-loop by exchanging heavy messenger fields with nonzero charges in both the SM and the dark sector gauge group. Alternatives can be considered for the gauge group from the dark sector; however, the most straightforward choice is an additional $U(1)'$ gauge group with abelian symmetry. The corresponding gauge boson is the dark photon [63]. Such a portal model is not new to the literature and has been studied since the 1980s [64, 65, 66, 67]. Since a vector portal model is created and examined in depth in Chapter 4, this part is included superficially for the sake of completeness in order not to fall into repetition.

CHAPTER 4

THE SM AND HIDDEN SECTOR WITH ABELIAN GAUGE GROUP

The distinction of light particles is constrained by the sensitivity of the detectors employed in hadron colliders, which limits the masses of particles that can be probed. As a result, experiments with high luminosity rather than high energy may be used to observe light particles. In recent years, the research on light-mass gauge bosons has gained particular importance. These bosons can exist in a dark/hidden sector and interact with the SM through portals. The most well-known of these portals is the abelian vector portal, and the gauge group is $U(1)_{B-L}$. There may be a kinetic mixing between this gauge group and the hyperweak abelian group $U(1)_Y$ of the SM that does not violate the gauge symmetries. In addition to the kinetic mixing, mass mixing between fields by the Higgs field may be feasible, but it is out of the scope of this study. Gauge sector, mass gain mechanism, and the interaction Lagrangian are the three key concepts that can be considered when analyzing the model. Below, these are taken into account as a whole. If we focus on the parts of the SM that are affected and changed by this new sector, the relevant Lagrangians are written as follows[1][2][3]

$$\mathcal{L}_{\text{Gauge}} = \mathcal{L}^{\text{KE}}_{\text{Gauge}} + \mathcal{L}^{\text{KM}}_{\text{Gauge}} + \mathcal{L}^{\text{Mass}}_{\text{Gauge}} \tag{4.1}$$

$$\mathcal{L}^{\text{KE}}_{\text{Gauge}} = -\frac{1}{4} W_{3\mu\nu} W_3^{\mu\nu} - \frac{1}{4} Y_{\mu\nu} Y^{\mu\nu} - \frac{1}{4} X^0_{\mu\nu} X^{0\mu\nu} + ... \tag{4.2}$$

$$\mathcal{L}^{\text{KM}}_{\text{Gauge}} = -\frac{1}{2} \sin\epsilon X^0_{\mu\nu} Y^{\mu\nu} \tag{4.3}$$

[1] In fact, if the most general gauge sector is written, the coefficient of each term in the $\mathcal{L}^{\text{KE}}_{\text{Gauge}}$ can be taken as a, b, and c, respectively. By rescaling the gauge fields and canonicalizing the kinetic energy terms, the above form is obtained with $a = b = 1$ and $c = \sin\epsilon$.

[2] In $\mathcal{L}^{\text{Mass}}_{\text{Gauge}}$, the mass term belonging to the dark sector may have emerged through a Higgs mechanism existing in that sector or by the Stueckelberg mechanism. The other mass term arises after the symmetry breaking through the Higgs doublet in the Standard Model and cannot be explicitly added to the Lagrangian in the first place. This situation will be concerned further below.

[3] $\mathcal{L}_{\text{int}}$ will be discussed later.

$$\mathcal{L}^{\text{Mass}}_{\text{Gauge}} = \frac{1}{2}m_X^2 X^0_\mu X^{0\mu} + \frac{1}{2}m_{W_3} W_{3\mu} W_3^\mu + ... \tag{4.4}$$

$$\mathcal{L}_{\text{int}} = \sum_i \bar{f}_i i \not{D} f_i \tag{4.5}$$

Here, the kinetic energies of $W_{3\mu}$ from $SU(2)_L$ group, Y_μ from $U(1)_Y$ and X^0_μ gauge bosons from $U(1)_{B-L}$ and field strength tensors are given. Due to the gauge symmetry, kinetic mixing (KM) can only be possible between the hypercharge field, Y_μ, and the dark sector gauge field, X^0_μ, and this kinetic mixing coupling is expressed by the parameter $\sin\epsilon$. Of course, if the KM is taken as very small, it will be in the form of $\sin\epsilon \simeq \epsilon$. In addition, the mass of the dark sector gauge boson is expressed as m_X.

By keeping the KM term as it is, the theory can be developed on the basis of these gauge fields, and the calculations can be made accordingly, or alternatively, such mixings can be eliminated by employing a new basis. To show this; it can be transformed from $(Y_\mu, W_{3\mu}, X^0_\mu)$ to another gauge basis $(B_\mu, W_{3\mu}, X_\mu)$ with a transformation as follows[4]

$$\begin{pmatrix} B_\mu \\ W_{3\mu} \\ X_\mu \end{pmatrix} = \begin{pmatrix} 1 & 0 & \sin\epsilon \\ 0 & 1 & 0 \\ 0 & 0 & \cos\epsilon \end{pmatrix} \begin{pmatrix} Y_\mu \\ W_{3\mu} \\ X^0_\mu \end{pmatrix} = V_{BX,YX^0}. \begin{pmatrix} Y_\mu \\ W_{3\mu} \\ X^0_\mu \end{pmatrix} \tag{4.6}$$

On this new basis, the KM term in the $\mathcal{L}^{\text{KM}}$ is no longer present, but this transformation will change both the mass and interaction terms. Therefore, it is necessary to make additional transformations to reach the physical gauge bosons in the mass-basis, and this is related to the symmetry-breaking step and the mass acquisition mechanism.

Currently, regardless of the presence of the dark sector, there is a symmetry-breaking mechanism of the form $G_{\text{SM}} \to SU(3)_C \otimes SU(2)_L \otimes U(1)_{em}$, where $U(1)_{em}$ represents the electromagnetic interactions that remain unbroken. To clarify the situation, one can define the covariant derivative for the $G_{\text{SM}} \otimes U(1)_{B-L}$ model as:

$$\begin{aligned} D_\mu &= \partial_\mu - ig_W \mathbf{t}.\mathbf{W}_\mu - ig_Y Y Y_\mu - ig_{BL} Q_D X^0_\mu \\ &= \partial_\mu - ig_W t_3 W_{3\mu} - ig_Y Y Y_\mu - ig_{BL} Q_D X^0_\mu + [-i\frac{g_W}{\sqrt{2}}(t_+ W^+_\mu + t_- W^-_\mu)] \\ &= -ig_W t_3 W_{3\mu} - ig_Y Y B_\mu - \frac{i}{\cos\epsilon}(-g_Y Y \sin\epsilon + g_{BL} Q_D) X_\mu + ... \end{aligned} \tag{4.7}$$

Besides the inclusion of coupling constants of gauge groups in the covariant derivative; t_3 (weak isospin), Y (weak hypercharge), and Q_D (dark charge) represent the

[4] Although it does not mix with other gauge fields, $W_{3\mu}$ is introduced here for later purposes.

charge operators under $SU(2)_L$, $U(1)_Y$, and $U(1)_{B-L}$, respectively. Furthermore, since the term enclosed in square brackets in the second line will not be affected by the presence of $U(1)_{B-L}$, that term is not explicitly stated in the third line and the following steps.

To elaborate on the mass acquisition mechanism, if a Higgs doublet field, H, with weak hypercharge $Y(H) = 1/2$ is defined, the vev of this field can be expressed as $\langle H \rangle = \begin{pmatrix} 0 & v/\sqrt{2} \end{pmatrix}^T$ (it can also be expressed as $v = 246$ GeV here). Then the mass terms can be written as[5]

$$\begin{aligned} \mathcal{L}^{\text{Mass}}_{\text{Gauge}} &= \frac{1}{2} m_X^2 X^0_\mu X^{0\mu} + (D_\mu \langle H \rangle)(D^\mu \langle H \rangle)^\dagger \\ &= \frac{1}{2} m_X^2 \sec^2 \epsilon X_\mu X^\mu \\ &+ \frac{1}{8}(g_Y^2 + g_W^2) v^2 (-\sin\theta_W B_\mu + \cos\theta_W W_{3\mu} + \tan\epsilon \sin\theta_W X_\mu)^2 \end{aligned} \tag{4.8}$$

where the Weinberg mixing angle here is defined as usual without considering new contributions, $\tan\theta_W \equiv g_Y/g_W$. If there was no X_μ field (or $\epsilon \to 0$), the resulting term $-\sin\theta_W B_\mu + \cos\theta_W W_{3\mu}$ would normally be the Z boson, and the other orthogonal state, $\cos\theta_W B_\mu + \sin\theta_W W_{3\mu}$, would be the photon. Of course, the gauge fields obtained with X_μ are no longer physical, and as can be understood from equation 4.8, a final transformation is required. As an intermediate step, without changing X_μ, this can be achieved by moving from $(B_\mu, W_{3\mu}, X_\mu)$ to $(\widetilde{B}_\mu \equiv A_\mu, \widetilde{W}_{3\mu}, X_\mu)$ basis as

[5] Since the quantum charge of the Higgs doublet under $U(1)_{B-L}$ is zero ($Q_D(H) = 0$), it does not contribute to the mass-square matrix, and no additional mass term appears for the X_μ field via the Higgs mechanism.

follows[6]

$$\begin{aligned}
\begin{pmatrix} A_\mu \\ \widetilde{W}_{3\mu} \\ X_\mu \end{pmatrix} &= \begin{pmatrix} \cos\theta_W & \sin\theta_W & 0 \\ -\sin\theta_W & \cos\theta_W & 0 \\ 0 & 0 & 1 \end{pmatrix} \begin{pmatrix} B_\mu \\ W_{3\mu} \\ X_\mu \end{pmatrix} \\
&\equiv V_{A\widetilde{W},BW} \cdot \begin{pmatrix} B_\mu \\ W_{3\mu} \\ X_\mu \end{pmatrix} \\
&= V_{A\widetilde{W},BW} . V_{BX,YX^0} \cdot \begin{pmatrix} Y_\mu \\ W_{3\mu} \\ X^0_\mu \end{pmatrix} \qquad (4.9) \\
&\equiv V_{A\widetilde{W},YX^0} \cdot \begin{pmatrix} Y_\mu \\ W_{3\mu} \\ X^0_\mu \end{pmatrix} \\
&= \begin{pmatrix} \cos\theta_W & \sin\theta_W & \sin\epsilon\cos\theta_W \\ -\sin\theta_W & \cos\theta_W & -\sin\epsilon\sin\theta_W \\ 0 & 0 & \cos\epsilon \end{pmatrix} \begin{pmatrix} Y_\mu \\ W_{3\mu} \\ X^0_\mu \end{pmatrix}
\end{aligned}$$

The V_{BX,YX^0} matrix here is defined in equation 4.6. Similarly, the $V_{A\widetilde{W},BW}$ matrix and the $V_{A\widetilde{W},YX^0}$ matrix that transforms from the first basis to the last one are also defined. The basis obtained after transformations $(A_\mu, \widetilde{W}_{3\mu}, X_\mu)$ is not the same as the mass basis because all terms are not diagonalized, as can be seen from the following equation. If we express equation 4.8 on this basis:

$$\mathcal{L}^{\text{Mass}}_{\text{Gauge}} \equiv \frac{1}{2} \begin{pmatrix} A_\mu & \widetilde{W}_{3\mu} & X_\mu \end{pmatrix} . \mathcal{M}^2_{\text{Gauge}} \cdot \begin{pmatrix} A_\mu \\ \widetilde{W}_{3\mu} \\ X_\mu \end{pmatrix} \qquad (4.10)$$

where

$$\mathcal{M}^2_{\text{Gauge}} = \begin{pmatrix} 0 & 0 & 0 \\ 0 & m^2_{W_3} & m^2_{W_3} \tan\epsilon \sin\theta_W \\ 0 & m^2_{W_3} \tan\epsilon \sin\theta_W & m^2_X \sec^2\epsilon + (m_{W_3} \tan\epsilon \sin\theta_W)^2 \end{pmatrix} \qquad (4.11)$$

It is clear that the photon has zero mass in the most recent $\mathcal{M}^2_{\text{Gauge}}$ mixing matrix, but the mass-square terms of the remaining $(W_{3\mu}, X_\mu)$ fields are still not diagonal. If an

[6] As can be seen from the results given below, since $\widetilde{B}_\mu \equiv A_\mu$ is equal to the physical photon field, the A_μ photon field is employed directly.

orthogonal transformation is made at this point,

$$\begin{aligned}
\begin{pmatrix} A_\mu \\ Z_\mu \\ A'_\mu \end{pmatrix} &= \begin{pmatrix} 1 & 0 & 0 \\ 0 & \cos\beta & \sin\beta \\ 0 & -\sin\beta & cos\beta \end{pmatrix} \begin{pmatrix} A_\mu \\ \widetilde{W}_{3\mu} \\ X_\mu \end{pmatrix} \\
&\equiv V_{ZA',\widetilde{W}X} \cdot \begin{pmatrix} A_\mu \\ \widetilde{W}_{3\mu} \\ X_\mu \end{pmatrix} \\
&= V_{ZA',\widetilde{W}X} . V_{A\widetilde{W},BW} . V_{BX,YX^0} \cdot \begin{pmatrix} Y_\mu \\ W_{3\mu} \\ X^0_\mu \end{pmatrix} \\
&\equiv V_{AZA',YWX^0} \cdot \begin{pmatrix} Y_\mu \\ W_{3\mu} \\ X^0_\mu \end{pmatrix} \\
&= \begin{pmatrix} \cos\theta_W & \sin\theta_W & \sin\epsilon\cos\theta_W \\ -\cos\beta\sin\theta_W & \cos\beta\cos\theta_W & \sin\beta\cos\epsilon - \cos\beta\sin\epsilon\sin\theta_W \\ \sin\beta\sin\theta_W & -\sin\beta\cos\theta_W & \cos\beta\cos\epsilon + \sin\beta\sin\epsilon\sin\theta_W \end{pmatrix} \begin{pmatrix} Y_\mu \\ W_{3\mu} \\ X^0_\mu \end{pmatrix}
\end{aligned} \tag{4.12}$$

and using this basis, if equation 4.8 is rewritten and the angle β is chosen accordingly to obtain[7]

$$\mathcal{L}^{\text{Mass}}_{\text{Gauge}} = \frac{1}{2} \begin{pmatrix} A_\mu & Z_\mu & A'_\mu \end{pmatrix} \begin{pmatrix} 1 & 0 & 0 \\ 0 & m_Z^2 & 0 \\ 0 & 0 & m_{A'}^2 \end{pmatrix} \begin{pmatrix} A_\mu \\ Z_\mu \\ A'_\mu \end{pmatrix} \tag{4.13}$$

It was initially suggested that three primary categories would be used to analyze the effect of the new sector on the SM. The interaction Lagrangian is the missing piece

[7] The explicit form of this parameter is $\tan\beta = m^2_{W_3} \tan\epsilon \sin\theta_W / (m^2_{W_3} - m^2_{A'})$.

so far. Examining the fermion kinetic term is all that is needed to complete this.

$$
\begin{aligned}
\mathcal{L}_{\text{int}} &= \sum_i \bar{f}_i i \not{D} f_i \\
&= \sum_i \bar{f}_i (g_W t_{3i} W_{3\mu} + g_Y Y_i Y_\mu + g_D Q_{Di} X^0_\mu) \gamma^\mu f_i \\
&\equiv g_Y j^\mu_Y Y_\mu + g_W j^\mu_3 W_{3\mu} + g_D j^\mu_X X^0_\mu \\
&= \begin{pmatrix} g_Y j^\mu_Y & g_W j^\mu_3 & g_D j^\mu_X \end{pmatrix} \begin{pmatrix} Y_\mu \\ W_{3\mu} \\ X^0_\mu \end{pmatrix} \\
&= \begin{pmatrix} g_Y j^\mu_Y & g_W j^\mu_3 & g_D j^\mu_X \end{pmatrix} . V^{-1}_{AZA',YWX^0} . \begin{pmatrix} A_\mu \\ Z_\mu \\ A'_\mu \end{pmatrix}
\end{aligned}
\tag{4.14}
$$

Here, the inverse of the total transformation matrix (V^{-1}_{AZA,YX^0}), which is explicitly given in equation 4.12, is employed. The SM fermion currents with hypercharge, weak force and dark force are also expressed above as j^μ_Y, j^μ_3, and j^μ_X, respectively, and their definitions can be seen in the second line.

When the terms given in equation 4.14 are calculated explicitly, the new interaction vertices such as $\bar{f} f A'_\mu$ as well as the interaction vertices such as $\bar{f} f Z_\mu$ in the SM will change. It would not be illuminating to state these interactions for the general case of mixing angles described earlier. For example, at a limit where the kinetic mixing parameter (ϵ) is non-zero, where the other coupling from the dark sector (g_D) is zero, together with $\epsilon \ll 1$ ($\sin\epsilon \to \epsilon$) and $m_{A'} \ll m_Z$, $\mathcal{L}_{\bar{f}fA'}$ takes the following form:

$$
\mathcal{L}_{\bar{f}fA'} = \epsilon \cos\theta_W Q_{em} \bar{f} \gamma^\mu f A'_\mu \equiv Q_{\text{millicharge}} \bar{f} \gamma^\mu f A'_\mu \tag{4.15}
$$

In this case, since the access to the SM fermions from the dark sector is only via kinetic mixing with the photon, they acquire extremely small millicharges ($Q_{\text{millicharge}} \equiv \epsilon \cos\theta_W Q_{em}$) from the dark photon in addition to their own electromagnetic charge (Q_{em}). The mixing of the dark photon with $W_{3\mu}$ in the electroweak sector is often neglected; therefore, the coefficient of Q_{em} is taken as ϵ. In this context, taking $\theta_W \to 0$ in $Q_{\text{millicharge}}$ gives the same result.

CHAPTER 5

COMPACT LINEAR COLLIDER

The Compact Linear Collider (CLIC) is a proposed multi-TeV electron-positron linear collider that is planned to be constructed at CERN, a research organization located on the border between France and Switzerland. This chapter will discuss the design of CLIC and the potential for researching new physics at the collider.

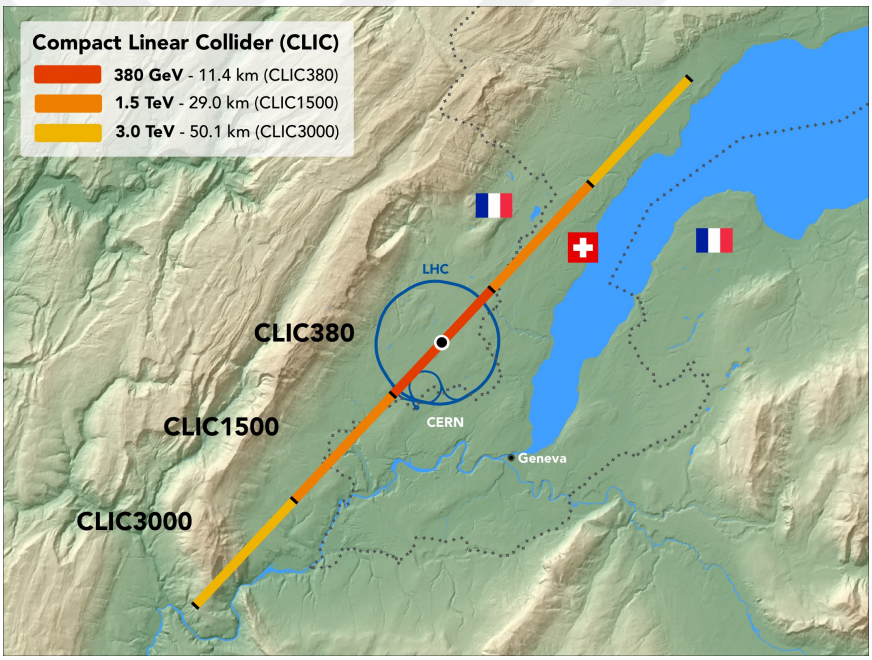


Figure 5.1: The footprint of a future CLIC accelerator with energy stages of 380 GeV, 1.5 TeV and 3 TeV (Image credit: CERN)

CLIC is designed to produce high-energy head-on collisions between electrons and positrons, and it is expected to be constructed and operated in three stages with collision energies of 380 GeV, 1.5 TeV, and 3 TeV. The high collision energy, large luminosity, and clean environment for e^+e^- collisions at CLIC will enable the precise

measurement of the properties of Standard Model particles such as the Higgs boson and the top quark. Additionally, CLIC has the potential to discover indirect effects of new physics by testing the parameters of the Standard Model Effective Field Theory with high precision. CLIC is expected to have a wider reach into physics beyond the Standard Model than the High-Luminosity Large Hadron Collider (HL-LHC), including the ability to study newly discovered particles that exhibit non-standard signatures. The CLIC physics program is expected to make significant progress in advancing our understanding of the unresolved questions in particle physics [68].

CLIC will be built in stages with increasing center-of-mass energies in order to maximize the number of potential physics applications. The higher-energy stages, which are currently expected to be at 1.5 TeV and 3 TeV, offer a unique sensitivity for many new physics scenarios. The parameters for each distinct energy state are listed in Table 5.1 [69].

Table 5.1: Parameters of the CLIC energy stages.

Parameter	**Symbol**	**Unit**	**Stage 1**	**Stage 2**	**Stage 3**
Center-of-mass energy	$\sqrt{s}$	GeV	380	1500	3000
Repetition frequency	f_{rep}	Hz	50	50	50
Number of bunches per train	n_{b}		352	312	312
Bunch separation	Δt	ns	0.5	0.5	0.5
Pulse length	τ_{RF}	ns	244	244	244
Accelerating gradient	G	MV/m	72	72/100	72/100
Total luminosity	$\mathscr{L}$	$10^{34}\text{cm}^{-2}\text{s}^{-1}$	1.5	3.7	5.9
Luminosity above 99% of $\sqrt{s}$	$\mathscr{L}_{0.01}$	$10^{34}\text{cm}^{-2}\text{s}^{-1}$	0.9	1.4	2
Total integrated luminosity per year	$\mathscr{L}_{\text{int}}$	fb^{-1}	180	444	708
Main linac tunnel length		km	11.4	29.0	50.1
Number of particles per bunch	N	10^9	5.2	3.7	3.7
Bunch length	σ_z	µm	70	44	44
IP beam size	σ_x/σ_y	nm	149/2.9	$\sim 60/1.5$	$\sim 40/1$
Normalized emittance (end of linac)	$\varepsilon_x/\varepsilon_y$	nm	900/20	660/20	660/20
Final RMS energy spread		%	0.35	0.35	0.35
Crossing angle (at IP)		mrad	16.5	20	20

The present CLIC baseline staging scenario, which is based on accelerator ramp-

up and up-time scenarios that have been coordinated with those of other potential future colliders, anticipates that the three energy stages, $\sqrt{s} = 380$ GeV, 1.5 TeV and 3 TeV, of the collider will have 1.0 ab^{-1}, 2.5 ab^{-1}, and 5.0 ab^{-1} of luminosity, respectively. According to the baseline scenario, the electron beam is expected to be polarized by $\pm 80\%$ along its longitudinal axis, but positron polarization is not available. At the early energy stage, equal proportions of -80% and +80% polarization running are anticipated [68]. Above the 1 TeV energy stages, it is expected that the collected luminosities will be split in a ratio of 80:20 during operation with -80% and +80% electron beam polarization. The use of polarized beams can provide additional information about the interactions being studied and can improve the sensitivity of certain measurements. The CLIC baseline staging scenario has been designed to maximize the potential physics applications of the collider and to optimize the use of the available luminosity [70].

5.1 New Physics Searches at CLIC

Extensive documentation in the literature and summaries in [71, 72, 73] highlight the CLIC's ability to investigate concrete new physics scenarios that address several major unsolved topics in particle physics. CLIC is able to probe electroweak charged particles on the scale of TeV, or more generally, particles that interact with the Standard Model with electroweak-sized couplings. This is much beyond the capability of the HL-LHC. At the CLIC, it is possible to produce any such new particle at a sizeable rate up to the kinematic limit of 1.5 TeV and, in some circumstances, up to 3 TeV, using only a single production mechanism. Different algorithms can be employed depending on the decay channel. New particles generate signals that can be easily separated from backgrounds as they decay into conventional final states that produce prompt jets, leptons, and photons. Backgrounds from SM processes typically have comparable cross sections to the signal since the same electroweak interactions generate them. This is the primary advantage of lepton colliders over hadron colliders, allowing the CLIC to perform better than the HL-LHC. In the majority of instances, the signals can be isolated so that new particle properties can be measured precisely, and BSM scenarios may be tested by comparing their predictions on particle proper-

ties. The potential for CLIC to directly investigate new physics is well described in the scientific literature, particularly in [71, 73, 74].

CHAPTER 6

NUMERICAL ANALYSIS

6.1 Some Kinematical Variables

In high-energy particle physics, collider experiments involve the study of high-energy particle collisions using accelerators such as the Compact Linear Collider (CLIC) at CERN. These collisions can produce a wide variety of particles, each with its own unique properties and behaviors. In order to understand and analyze the results of these experiments, various parameters are used to describe the properties and behavior of the particles involved. Some of the key parameters used in collider experiments and hence in the analysis of the study within this thesis can be explained as follows.

Missing transverse energy refers to the energy that is not observed in an experiment, usually due to the presence of invisible particles such as neutrinos. It can be represented as $\not{E}_T = \sqrt{\sum E_x^2 + \sum E_y^2}$, where E_x and E_y are the energy of each particle in the perpendicular plane to the beamline. By measuring the missing transverse energy in a collision, one can infer the existence of particles too massive or too short-lived to be detected directly. This can help physicists discover new particles or phenomena that may not have been observed before.

Transverse momentum refers to the momentum of a particle in the plane perpendicular to the beam direction. It can be denoted as $p_T = \sqrt{(p_x^2 + p_y^2)}$, where p_x and p_y are the momentum components in the x and y directions, respectively. Measuring the transverse momentum of particles produced in a collision can help to understand the properties of the particles, such as their mass and their interactions with other particles. Besides, transverse momentum reveals what happens directly at the vertex, whereas momentum along the beamline may be leftover from the beam particles.

Pseudorapidity is a measure of the angle of a particle's trajectory relative to the beam direction, defined as $\eta = -\ln\tan(\theta/2)$, where θ is the polar angle of the particle's momentum vector. Measuring the pseudorapidity of particles produced in a collision can help to understand the collision's kinematics, such as the energy and momentum of the particles.

Transverse mass is a measure of the mass of a particle based on its transverse and longitudinal momentum (momentum along the beam direction). It can be defined as $m_T = \sqrt{(p_T^2 + m^2)}$, where m is the particle's mass. It is also used in collider experiments to study the properties of particles, such as their mass and interactions with other particles.

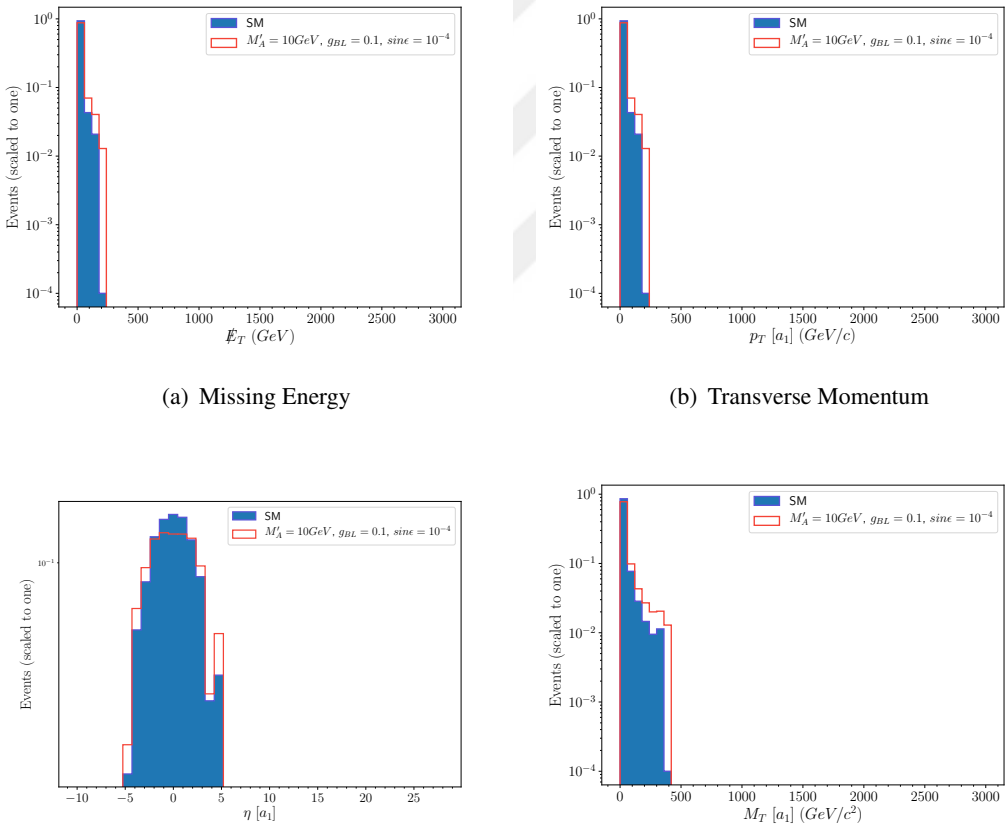
6.2 Madgraph Simulation Results

6.2.1 DP Only Case

As described in the previous chapter, the Compact Linear Collider (CLIC) is a suitable electron-positron collider that can operate up to 3 TeV center of mass energies in the future. CLIC will be built in stages using a plan that operates at center-of-mass energy levels of 380 GeV, 1.5 TeV, and 3 TeV. Even though it will also focus on a wide range of Standard Model studies, such as the direct measurement of Higgs self-coupling and top-quark Yukawa coupling, primarily while operating at the last two energy phases, its main goal will be to look for new physics that goes beyond the Standard Model. Compared to hadron colliders, the low background conditions at CLIC provide rich exploration potential. Therefore, a background-free "clean environment" and a simple signal will be the prominent features of CLIC to achieve its goal. The most general approach for dark photon and dark matter experiments in future e^-e^+ colliders is based on a mono-photon signal. In this context, dark photon contribution to mono-photon signal via $e^-e^+ \to \gamma\nu\nu$ process at 380 GeV, 1.5 TeV, and 3 TeV center of mass energy levels in CLIC are investigated. For these energy levels, contributions from both the SM (without the dark photon contribution), and the dark photon are obtained.

Table 6.1: Cross-section values of contributions from SM and dark photon (DP) to the mono-photon + missing energy signal ($e^-e^+ \to \gamma\nu_l\bar{\nu}_l$) at CLIC energy levels. The dark sector parameters are selected as $M'_A = 10$ GeV, $g_{B-L} = 0.1$ and $sin\epsilon = 10^{-4}$.

$\sqrt{s}$	$\sigma_{SM}(e^-e^+ \to \gamma\nu_l\bar{\nu}_l)[pb]$	$\sigma_{DP}(e^-e^+ \to \gamma\nu_l\bar{\nu}_l)[pb]$
380 GeV	8.25	11.03
1500 GeV	11.56	11.74
3000 GeV	12.98	13.04



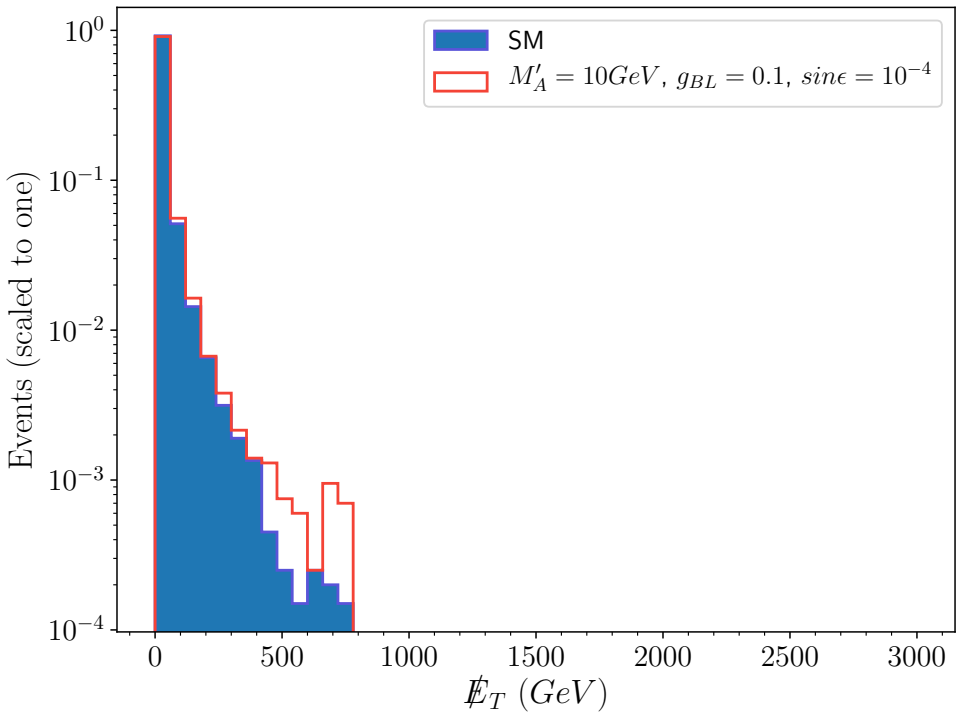
(a) Missing Energy

(b) Transverse Momentum

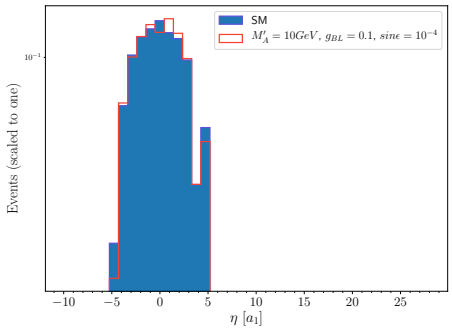
(c) Pseudorapidity

(d) Transverse Mass

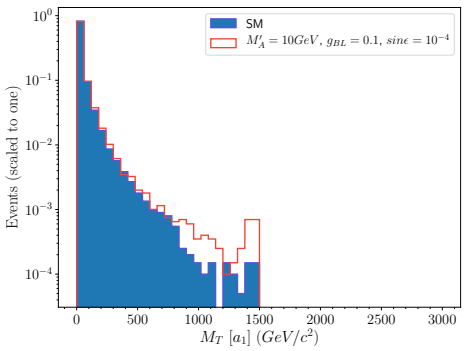
Figure 6.1: Distribution of events according to some variables by using Pythia and Delphes at 380 GeV center of mass energy for the ($e^-e^+ \to \gamma\nu_l\bar{\nu}_l$) process in CLIC. ($e^-$,$e^+$) beam polarizations are taken as (-80%, -30%).



(a) Missing Energy



(b) Pseudorapidity



(c) Transverse Mass

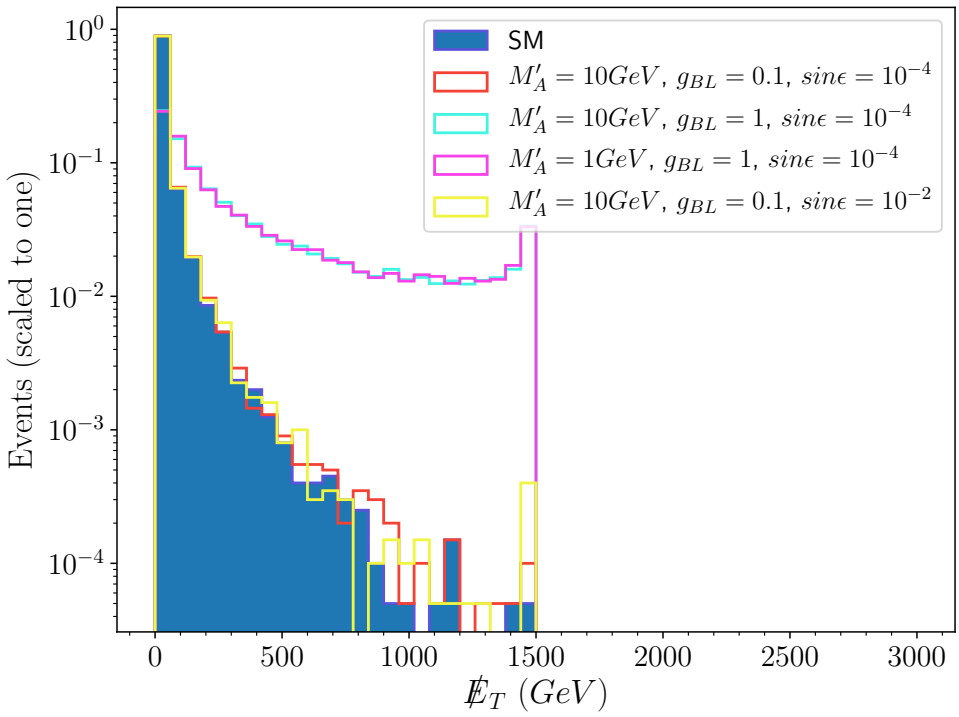
Figure 6.2: Distribution of events according to some variables by using Pythia and Delphes at 1500 GeV center of mass energy for the ($e^-e^+ \to \gamma\nu_l\bar{\nu}_l$) process in CLIC. ($e^-$,$e^+$) beam polarizations are taken as (-80%, -30%).

Table 6.2: Studied Parameters for the CLIC - Stage 3 (3 TeV)

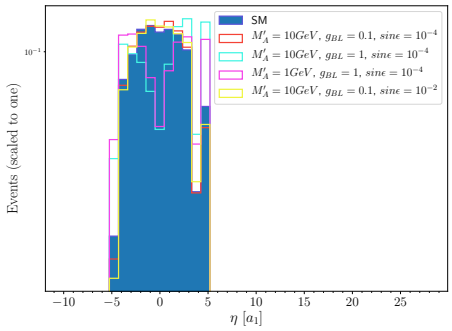
Case #	M'_A	g_{BL}	$sin\epsilon$
1	10 GeV	0.1	10^{-4}
2	10 GeV	1	10^{-4}
3	1 GeV	1	10^{-4}
4	10 GeV	0.1	10^{-2}

The analysis is studied with the help of Madgraph by expanding the parameters in the case of the 3 TeV center of mass energy, which corresponds to the 3rd stage of CLIC. The reason is that the maximum center-of-mass energy state that can reveal the potential of CLIC is thought to be worth looking into further. At this point, the relevant parameters have been selected, as shown in Table 6.2.

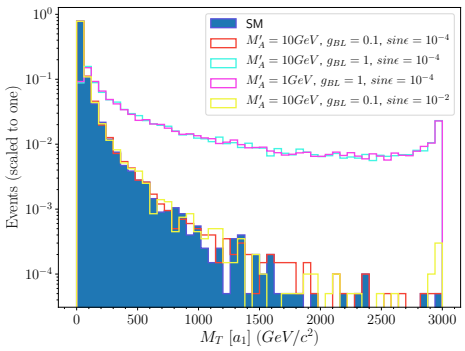
In the distributions examined for three different mass center energy stages of CLIC, it is observed that the most separation from the standard model is in the cases created for Stage 3. Especially cases where the coupling is set to 1 for a possible dark photon interaction yielded much more distinctive results for tracking dark photons in CLIC. On the other hand, the mass of the dark photon and kinetic mixing parameter do not appear to contribute significantly to this separation within the model framework.



(a) Missing Energy



(b) Pseudorapidity



(c) Transverse Mass

Figure 6.3: Distribution of events according to some variables by using Pythia and Delphes at 3000 GeV center of mass energy for the ($e^-e^+ \to \gamma\nu_l\bar{\nu}_l$) process in CLIC. ($e^-$,$e^+$) beam polarizations are taken as (-80%, -30%).

6.2.2 DP + DM Case

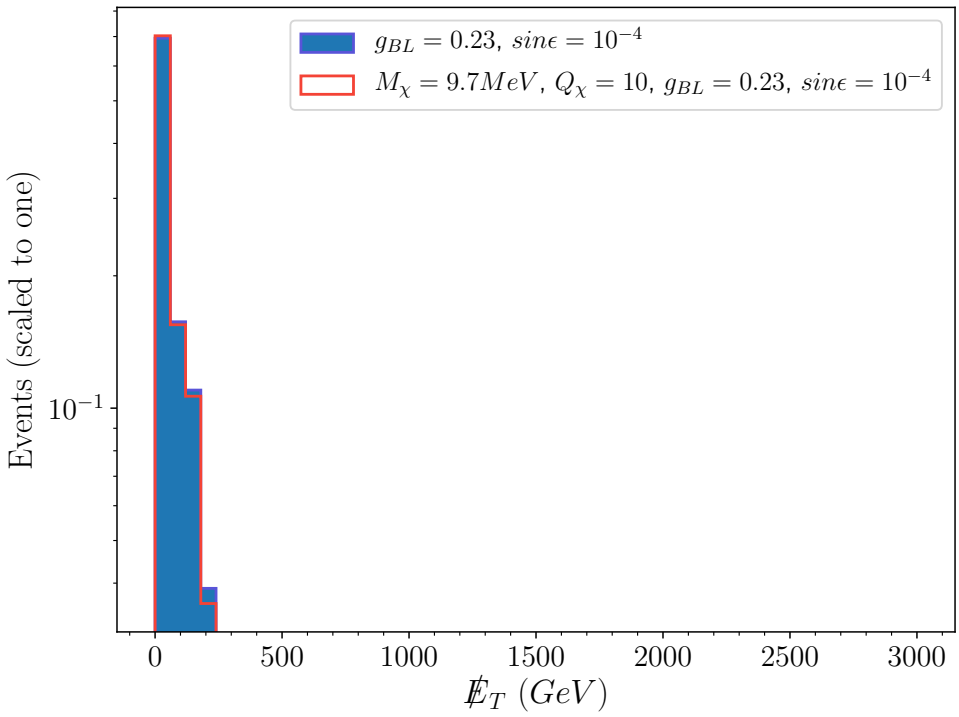
This section considers the two extreme cases for CLIC, Stage 1 and Stage 3, while also considering dark matter contributions. As the separation between the processes in which only the dark photon is involved and the processes in which dark matter contributions are taken into account cannot be observed clearly for Stage 1, it has been observed that this separation becomes more remarkable when Stage 3 is used. However, the selected parameter space can be accepted as a starting point and should be developed further.

Table 6.3: Cross-section values of contributions from DP and DP + DM processes to the mono-photon + missing energy signal ($e^-e^+ \to \gamma\nu_l\bar{\nu}_l$) at CLIC energy levels. The dark sector parameters are selected given in the Table 6.4.

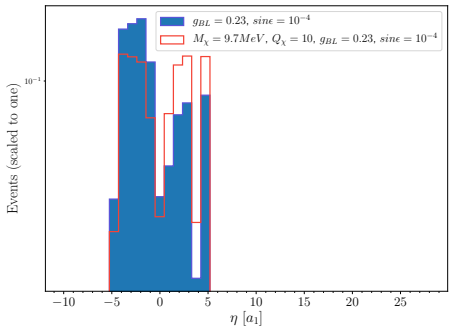
$\sqrt{s}$	$\sigma_{DP}(e^-e^+ \to \gamma\nu_l\bar{\nu}_l)[pb]$	$\sigma_{DP+DM}(e^-e^+ \to \gamma\chi\bar{\chi})[pb]$
380 GeV	2316	1.082×10^5
3000 GeV	39.46	1745

Table 6.4: Studied Parameters for DP + DM Case

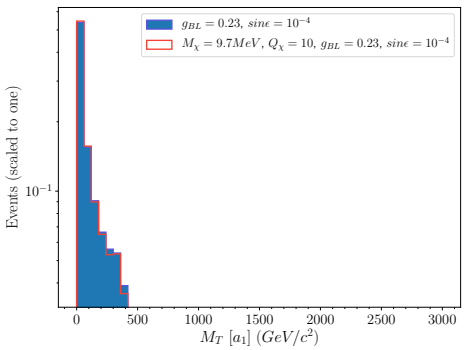
$\sqrt{s}$	M'_A	g_{BL}	$sin\epsilon$	M_{DM}	Q_{DM}
380 GeV (Stage 1)	10 GeV	0.1	10^{-4}	9.7 MeV	10
3000 GeV (Stage 3)	10 GeV	0.1	10^{-4}	9.7 MeV	10



(a) Missing Energy

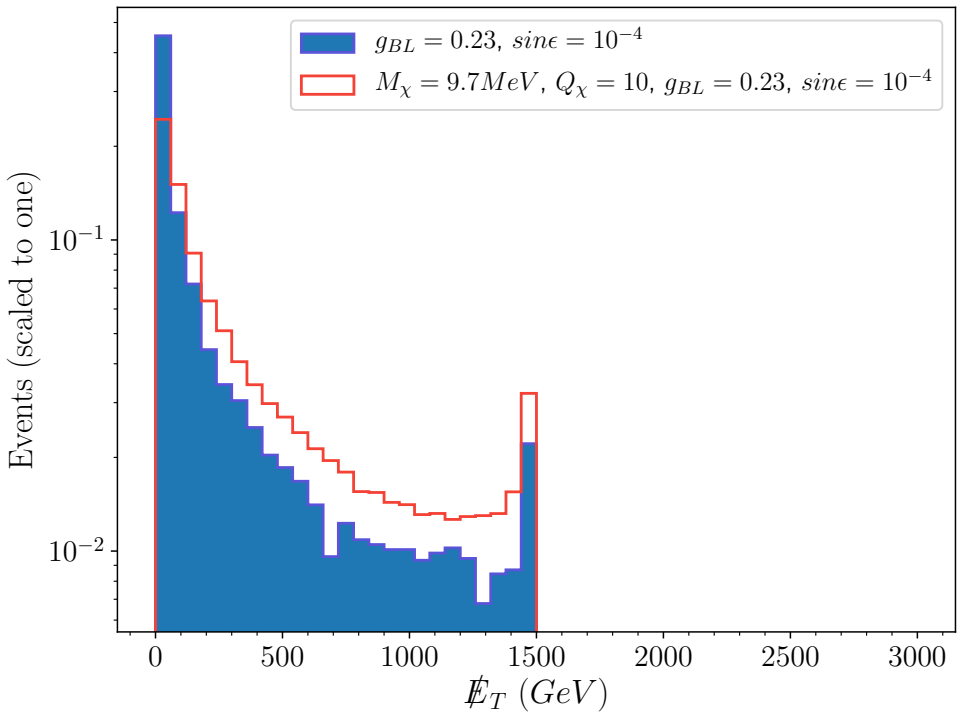


(b) Pseudorapidity

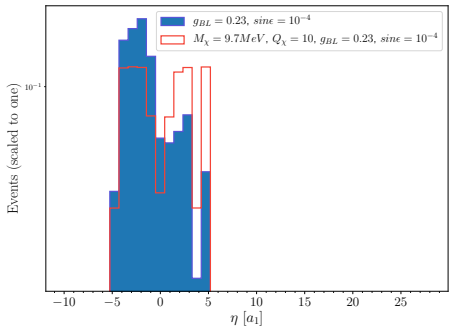


(c) Transverse Mass

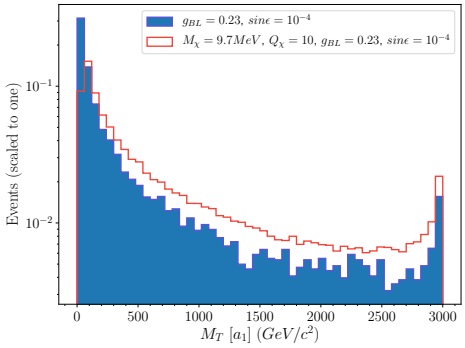
Figure 6.4: Distribution of events according to some variables by using Pythia and Delphes at 380 GeV center of mass energy for the ($e^-e^+ \rightarrow \gamma\chi\bar{\chi}$) process in CLIC. ($e^-$,$e^+$) beam polarizations are taken as (-80%, -30%).



(a) Missing Energy



(b) Pseudorapidity



(c) Transverse Mass

Figure 6.5: Distribution of events according to some variables by using Pythia and Delphes at 3000 GeV center of mass energy for the ($e^-e^+ \to \gamma\chi\bar{\chi}$) process in CLIC. ($e^-$,$e^+$) beam polarizations are taken as (-80%, -30%).

6.2.2.1 Relic Density Computation

In order to compute the relic density of the potential dark matter in the scenarios discussed, the MadDM package program was used together with MadGraph. First, an initial set of variables was used, and then these variables were iterated so that the calculated relic density would be compatible with that deduced from the Planck experiments. As can be seen from the graphs, although there is a slight separation for CLIC Stage 1, it has been found that this separation is much more prominent in Stage 3 runs. This may suggest that Stage 3 experiments with a 3 TeV center of mass energy may be more favorable in probing the potential dark matter.

The output of the MadDM can be seen below:

```
INFO: Start computing relic
maddm_card missed argument print_sigmas. Takes default: False
INFO: compilation done
INFO: MadDM Results
INFO:
****** Relic Density
OMEGA IS 0.120282
INFO: Relic Density       = 1.20e-01       WITHIN EXP ERROR
INFO: x_f                 = 1.20e+01
INFO: sigmav(xf)          = 1.12e-26 cm^3 s^-1
INFO: xsi                 = 1.00e+00
INFO:
INFO: Channels contributions:
INFO: chi chi~ > ve ve~   : 21.48 %
INFO: chi chi~ > vt vt~   : 21.48 %
INFO: chi chi~ > vm vm~   : 21.48 %
INFO: chi chi~ > u u~     : 7.14 %
INFO: chi chi~ > e- e+    : 21.47 %
INFO: chi chi~ > d d~     : 6.95 %
INFO: No contribution from processes: apap, zap, bb~, ss~,
zz, hap, zh, ta-ta+, tt~, cc~, w+w-, mu-mu+
```

CHAPTER 7

CONCLUSION

It is verified that the Standard Model is a powerful theory accurate to energies equivalent to those on the electroweak scale. The validity of the Standard Model may be extended thanks to recent developments in high-energy physics, which incorporate the model into ever more comprehensive frameworks. Studies are being conducted in great detail into the nature of the new physics. Although it is a widely held belief that new physics must exist outside the bounds of the Standard Model, it is possible to find clues to its existence at energies that are orders of magnitude lower than those predicted by the electroweak theory. As a result, in this thesis, we have searched for new physics that extends beyond the electroweak scale. More specifically, we have focused on the contribution of the dark photon to the distributions of possible events in CLIC.

In the first part of the thesis, a simulation is carried out for the CLIC at CERN. In this context, the center of mass energy was taken as 360 GeV, 1.5 TeV, and 3 TeV, respectively, and $e^-e^+ \to \gamma\nu\bar{\nu}$ process was investigated. Feynman diagrams of contributions from $e^-e^+ \to \gamma\nu\bar{\nu}$ in the framework of SM (which formed the background of the process of interest) and contributions from dark photon were determined, and these diagrams are included in the appendix. Different parameter values were used while computing the contributions from the dark photon. For these computations, the MadGraph package program was set to a 10 fb^{-1} luminosity state, and 20000 events were generated at the parton level. Event distributions belonging to the SM and the dark photon were shown in the previous chapter. The distribution for the dark photon processes at the hadron level according to the missing transverse energy was given, as well as the distributions of transverse momentum (p_T), transverse mass (M_T) and

pseudorapidity (η). In order to create these distributions and simulate the experimental environment more realistically, the hadronization and showering processes were created with the help of Pythia, the limitations of the collider were constructed with the help of Delphes, and then the distributions were obtained through MadAnalysis 5. The distributions obtained for the SM and the dark photon were plotted together, and in addition, the separation of the signal from the background and also the significance of the signal were calculated.

In the first place, when examining the mono-photon + missing energy situation, it was assumed that the missing energy was coming from neutrinos. Although this is normal in the Standard Model, dark matter is another critical source of missing energy in scenarios Beyond the Standard Model. In this sense, one of the ways to seek dark matter is to look at signals in the form of mono-photon + missing energy and evaluate the contribution from neutrinos as a background. In the first part of the analysis, only dark photon contributions were taken into account, and a similar analysis was later used to investigate the dark matter in colliders. For this part of the analysis, the existence of a fermion(dark fermion) from the hidden sector was considered and only allowed to interact with the dark photon. In the end, relic density computation is conducted with the MadDm package program's help. The relevant parameters for the prospective DM are selected accordingly to meet expectations from the Planck experiments.

The parameters used in this study are accepted as a starting point and are open to development. With further study and analysis, it is possible to construct a parameter space where much more separation from the SM can be observed.

REFERENCES

[1] C. P. Burgess and G. D. Moore, *The standard model : a primer.* Cambridge University Press, 2007.

[2] P. Langacker, *The standard model and beyond.* Series in high energy physics, cosmology, and gravitation, CRC Press/Taylor & Francis, 2010.

[3] G. Arnison, A. Astbury, B. Aubert, *et al.*, "Experimental observation of isolated large transverse energy electrons with associated missing energy at s=540 gev," *Physics Letters B*, vol. 122, no. 1, pp. 103–116, 1983.

[4] G. Arnison, A. Astbury, B. Aubert, *et al.*, "Experimental observation of lepton pairs of invariant mass around 95 gev/c2 at the cern sps collider," *Physics Letters B*, vol. 126, no. 5, pp. 398–410, 1983.

[5] A. Belloni, A. Freitas, J. Tian, *et al.*, "Report of the topical group on electroweak precision physics and constraining new physics for snowmass 2021," 2022.

[6] X. Wang, J. Chen, Y. Liu, *et al.*, "New gauge boson B_H production associated with w boson pair via $\gamma\gamma$ collision in the littlest higgs model," *Phys. Rev. D*, vol. 74, p. 015006, Jul 2006.

[7] I. Boiarska, K. Bondarenko, A. Boyarsky, *et al.*, "Phenomenology of gev-scale scalar portal," *Journal of High Energy Physics*, vol. 2019, no. 11, 2019.

[8] M. Blennow, E. Fernandez-Martinez, A. O.-D. Campo, *et al.*, "Neutrino portals to dark matter.," *European Physical Journal C: Particles and Fields*, vol. 79, no. 7, pp. 1 – 18, 2019.

[9] K. Fujikawa, "A Vector-Like Extension of the Standard Model," *Progress of Theoretical Physics*, vol. 92, pp. 1149–1160, 12 1994.

[10] S. Khalil, S. Moretti, D. Rojas-Ciofalo, and H. Waltari, "Monophoton signals at e+e- colliders in a simplified E6SSM," *Phys. Rev. D*, vol. 104, no. 3, p. 035008, 2021.

[11] A. C. Abusleme Hoffman *et al.*, "Detector Technologies for CLIC," 5 2019.

[12] N. Van Der Kolk, "CLIC Detector and Physics Status," tech. rep., CERN, Geneva, 2017. Talk presented at the International Workshop on Future Linear Colliders (LCWS2016), Morioka, Japan, 5-9 December 2016. C16-12-05.4.

[13] M. E. Peskin and D. V. Schroeder, *Introduction to quantum field theory.* Addison-Wesley Pub. Co., 1995.

[14] A. Dobado, *Effective Lagrangians for the standard model.* Texts and monographs in physics, Springer, 1997.

[15] J. F. Donoghue, B. R. Holstein, and E. Golowich, *Dynamics of the Standard Model.* No. Vol. 35 in Cambridge Monographs on Particle Physics, Nuclear Physics, and Cosmology, Cambridge University Press, 2nd ed., 2014.

[16] J. E. Dodd and B. Gripaios, *The Glashow–Weinberg–Salam Model*, p. 108–111. Cambridge University Press, 4 ed., 2020.

[17] S. L. Glashow, "Partial-symmetries of weak interactions," *Nuclear Physics*, vol. 22, no. 4, pp. 579–588, 1961.

[18] S. Weinberg, "A model of leptons," *Phys. Rev. Lett.*, vol. 19, pp. 1264–1266, Nov 1967.

[19] A. Salam, "Gauge Unification of Fundamental Forces," *Rev. Mod. Phys.*, vol. 52, pp. 525–538, 1980.

[20] F. Halzen and A. D. Martin, *Quarks and leptons : an introductory course in modern particle physics.* Wiley, 1984.

[21] M. Merk, I. van Vulpen, and W. Hulsbergen, "Particle physics 1." `https://www.nikhef.nl/~ivov/LectureNotes_SM_and_Higgs.pdf`, 2018.

[22] D. J. Gross and F. Wilczek, "Ultraviolet behavior of non-abelian gauge theories," *Phys. Rev. Lett.*, vol. 30, pp. 1343–1346, Jun 1973.

[23] S. Weinberg, "Non-abelian gauge theories of the strong interactions," *Phys. Rev. Lett.*, vol. 31, pp. 494–497, Aug 1973.

[24] C. Quigg, "Electroweak symmetry breaking and the Higgs sector," *Acta Phys. Polon. B*, vol. 30, pp. 2145–2192, 1999.

[25] S. Dawson, "Introduction to electroweak symmetry breaking," 1999.

[26] M. Spira and P. M. Zerwas, "Electroweak symmetry breaking and higgs physics," in *Computing Particle Properties* (H. Gausterer and C. B. Lang, eds.), (Berlin, Heidelberg), pp. 161–225, Springer Berlin Heidelberg, 1998.

[27] Y. Nagashima, *Beyond the Standard Model of Elementary Particle Physics.*, vol. 9783527411771. Osaka University: Wiley Blackwell, 2014.

[28] L. Hall, "Grand unification of effective gauge theories," *Nuclear Physics B*, vol. 178, no. 1, pp. 75–124, 1981.

[29] P. Langacker, "Grand unified theories and proton decay," *Physics Reports*, vol. 72, no. 4, pp. 185–385, 1981.

[30] H. Baer, V. Barger, P. Huang, *et al.*, "Radiative natural supersymmetry: Reconciling electroweak fine-tuning and the higgs boson mass," *Physical Review D*, vol. 87, no. 11, p. 115028, 2013.

[31] L. J. Hall and Y. Nomura, "A finely-predicted higgs boson mass from a finely-tuned weak scale," *Journal of High Energy Physics*, vol. 2010, no. 3, pp. 1–31, 2010.

[32] J. Jaeckel, V. M. Mehta, and L. T. Witkowski, "Musings on cosmological relaxation and the hierarchy problem," *Physical Review D*, vol. 93, no. 6, p. 063522, 2016.

[33] H.-Y. Cheng, "The strong cp problem revisited," *Physics Reports*, vol. 158, no. 1, pp. 1–89, 1988.

[34] B. Pontecorvo, "Neutrino experiments and the problem of conservation of leptonic charge," *Sov. Phys. JETP*, vol. 26, no. 984-988, p. 165, 1968.

[35] V. Gribov and B. Pontecorvo, "Neutrino astronomy and lepton charge," *Physics Letters B*, vol. 28, no. 7, pp. 493–496, 1969.

[36] M. Jeżabek and Y. Sumino, "Neutrino mixing and see-saw mechanism," *Physics Letters B*, vol. 440, no. 3-4, pp. 327–331, 1998.

[37] A. Sakharov, "Violation of cpin variance, casymmetry, and baryon asymmetry of the universe," *Sov. Phys. Usp*, vol. 34, p. 392, 1991.

[38] E. W. Kolb and M. S. Turner, "Grand unified theories and the origin of the baryon asymmetry," *Annual Review of Nuclear and Particle Science*, vol. 33, no. 1, pp. 645–696, 1983.

[39] T. Aoyama, N. Asmussen, M. Benayoun, *et al.*, "The anomalous magnetic moment of the muon in the standard model," *Physics reports*, vol. 887, pp. 1–166, 2020.

[40] J. P. Miller, E. de Rafael, and B. L. Roberts, "Muon (g- 2): experiment and theory," *Reports on Progress in Physics*, vol. 70, no. 5, p. 795, 2007.

[41] S. Hannestad and E. Mörtsell, "Probing the dark side: Constraints on the dark energy equation of state from cmb, large scale structure, and type ia supernovae," *Phys. Rev. D*, vol. 66, p. 063508, Sep 2002.

[42] R. Alonso, B. Grinstein, and J. M. Camalich, "Lepton universality violation with lepton flavor conservation in b-meson decays," *Journal of High Energy Physics*, vol. 2015, no. 10, pp. 1–30, 2015.

[43] C. Collaboration†‡, T. Aaltonen, S. Amerio, *et al.*, "High-precision measurement of the w boson mass with the cdf ii detector," *Science*, vol. 376, no. 6589, pp. 170–176, 2022.

[44] F. Zwicky, "Die rotverschiebung von extragalaktischen nebeln," *Helvetica physica acta*, vol. 6, pp. 110–127, 1933.

[45] V. C. Rubin and W. K. Ford Jr, "Rotation of the andromeda nebula from a spectroscopic survey of emission regions," *The Astrophysical Journal*, vol. 159, p. 379, 1970.

[46] Planck Collaboration, Adam, R., Ade, P. A. R., *et al.*, "Planck 2015 results - i. overview of products and scientific results," *A&A*, vol. 594, p. A1, 2016.

[47] Planck Collaboration, Ade, P. A. R., Aghanim, N., *et al.*, "Planck 2015 results - xiii. cosmological parameters," *A&A*, vol. 594, p. A13, 2016.

[48] M. Srednicki, R. Watkins, and K. A. Olive, "Calculations of relic densities in the early universe," *Nuclear Physics B*, vol. 310, no. 3-4, pp. 693–713, 1988.

[49] J. Beacham, C. Burrage, D. Curtin, *et al.*, "Physics beyond colliders at cern: Beyond the standard model working group report," *Journal of Physics. G: Nuclear and Particle Physics*, vol. 47, Jan. 2020.

[50] T. Lagouri, "Review on higgs hidden–dark sector physics at high-energy colliders," *Symmetry*, vol. 14, no. 7, p. 1299, 2022.

[51] P. Agrawal, M. Bauer, J. Beacham, *et al.*, "Feebly-interacting particles: Fips 2020 workshop report," *The European Physical Journal C*, vol. 81, no. 11, pp. 1–137, 2021.

[52] T. Yanagida, "Horizontal symmetry and masses of neutrinos," *Progress of Theoretical Physics*, vol. 64, no. 3, pp. 1103–1105, 1980.

[53] A. Boyarsky, J. Lesgourgues, O. Ruchayskiy, and M. Viel, "Realistic sterile neutrino dark matter with kev mass does not contradict cosmological bounds," *Phys. Rev. Lett.*, vol. 102, p. 201304, May 2009.

[54] M. B. Wise and Y. Zhang, "Stable bound states of asymmetric dark matter," *Phys. Rev. D*, vol. 90, p. 055030, Sep 2014.

[55] K. Petraki, L. Pearce, and A. Kusenko, "Self-interacting asymmetric dark matter coupled to a light massive dark photon," *Journal of Cosmology and Astroparticle Physics*, vol. 2014, p. 039, jul 2014.

[56] B. Batell, M. Pospelov, and A. Ritz, "Exploring portals to a hidden sector through fixed targets," *Phys. Rev. D*, vol. 80, p. 095024, Nov 2009.

[57] J. Alexander, M. Battaglieri, B. Echenard, *et al.*, "Dark sectors 2016 workshop: Community report," 2016.

[58] G. Aad, T. Abajyan, B. Abbott, *et al.*, "Observation of a new particle in the search for the standard model higgs boson with the atlas detector at the lhc," *Physics Letters B*, vol. 716, no. 1, pp. 1–29, 2012.

[59] S. Chatrchyan, V. Khachatryan, A. Sirunyan, *et al.*, "Observation of a new boson at a mass of 125 gev with the cms experiment at the lhc," *Physics Letters B*, vol. 716, no. 1, pp. 30–61, 2012.

[60] G. Lanfranchi, M. Pospelov, and P. Schuster, "The search for feebly interacting particles," *Annual Review of Nuclear and Particle Science*, vol. 71, no. 1, pp. 279–313, 2021.

[61] S. Alekhin, W. Altmannshofer, T. Asaka, *et al.*, "A facility to search for hidden particles at the cern sps: the ship physics case," *Reports on Progress in Physics*, vol. 79, p. 124201, oct 2016.

[62] D. Gorbunov and M. Shaposhnikov, "How to find neutral leptons of the νmsm?," *Journal of High Energy Physics*, vol. 2007, p. 015, oct 2007.

[63] S. Bilmiş, I. Turan, T. M. Aliev, *et al.*, "Constraints on dark photon from neutrino-electron scattering experiments," *Phys. Rev. D*, vol. 92, p. 033009, Aug 2015.

[64] L. B. Okun, "LIMITS OF ELECTRODYNAMICS: PARAPHOTONS?," *Sov. Phys. JETP*, vol. 56, p. 502, 1982.

[65] B. Holdom, "Two u(1)'s and ϵ charge shifts," *Physics Letters B*, vol. 166, no. 2, pp. 196–198, 1986.

[66] H. Goldberg and L. J. Hall, "A new candidate for dark matter," *Physics Letters B*, vol. 174, no. 2, pp. 151–155, 1986.

[67] P. Galison and A. Manohar, "Two z's or not two z's?," *Physics Letters B*, vol. 136, no. 4, pp. 279–283, 1984.

[68] P. Roloff, R. Franceschini, U. Schnoor, and A. Wulzer, "The compact linear e^+e^- collider (clic): Physics potential," 2018.

[69] A. Robson, P. N. Burrows, N. C. Lasheras, *et al.*, "The compact linear e^+e^- collider (clic): Accelerator and detector," 2018.

[70] T. K. Charles *et al.*, "The Compact Linear Collider (CLIC) - 2018 Summary Report," 12 2018.

[71] J. de Blas *et al.*, "The CLIC Potential for New Physics," 12 2018.

[72] E. Accomando *et al.*, "Physics at the CLIC multi-TeV linear collider," in *11th International Conference on Hadron Spectroscopy*, CERN Yellow Reports: Monographs, 6 2004.

[73] P. Lebrun, L. Linssen, A. Lucaci-Timoce, *et al.*, "The CLIC Programme: Towards a Staged e+e- Linear Collider Exploring the Terascale : CLIC Conceptual Design Report," 9 2012.

[74] "Physics and Detectors at CLIC: CLIC Conceptual Design Report," 2 2012.

APPENDIX A

FEYNMAN DIAGRAMS

A.1 Feynman Diagrams at SM Level

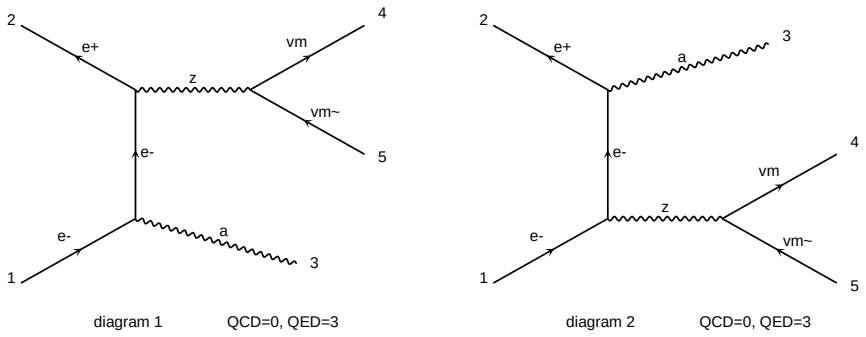


Figure A.1: 1st set of diagrams of the process: $e^{-}e^{+} > \gamma\nu_{\mu}\bar{\nu}_{\mu}$

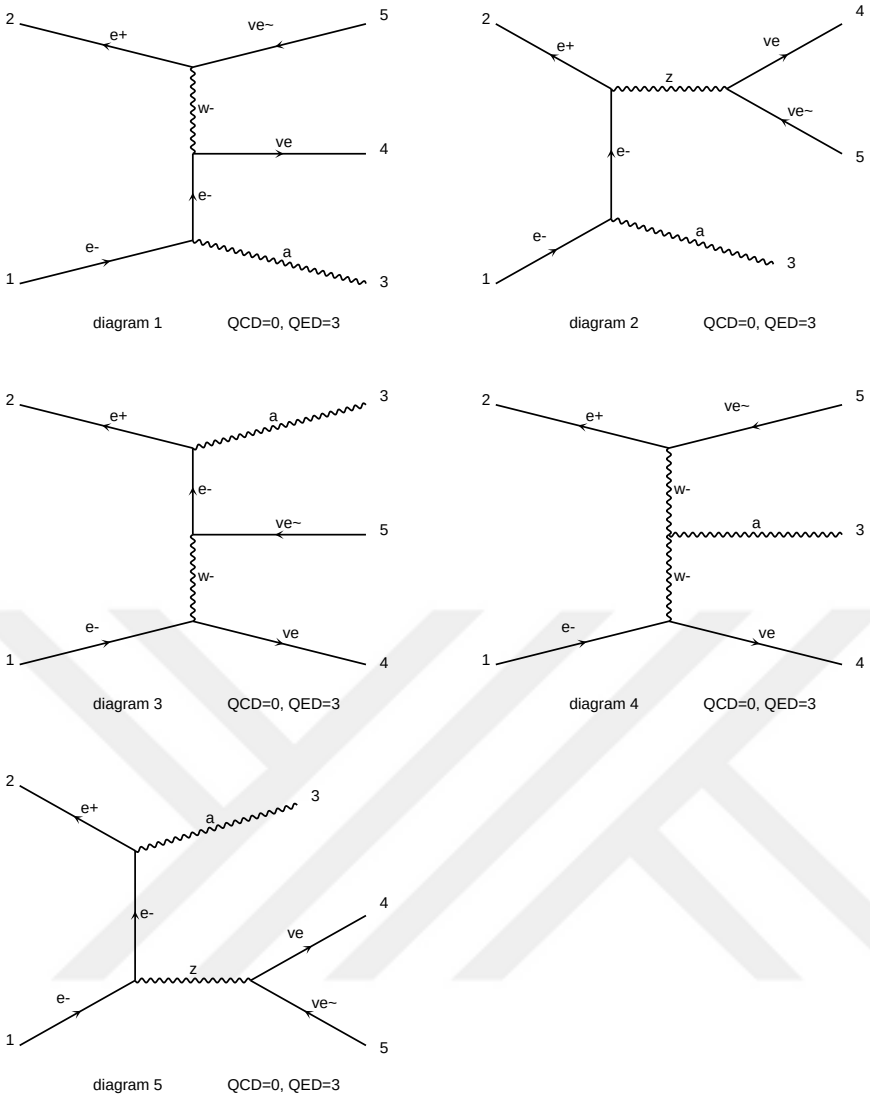


Figure A.2: 1st set of diagrams of the process: $e^- e^+ > \gamma \nu_e \bar{\nu}_e$

A.2 Feynman Diagrams with Hidden Sector Contribution (DP Only)

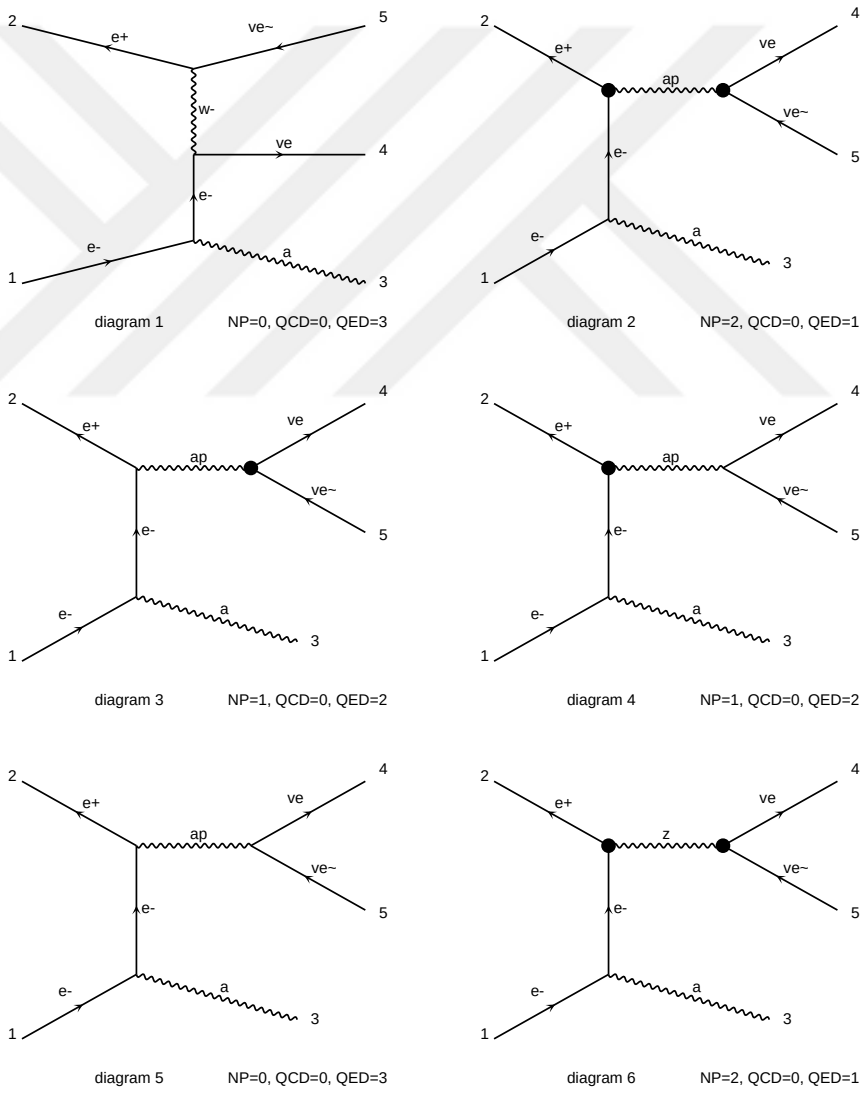


Figure A.3: 1st set of diagrams of the process: $e^{-}e^{+} > \gamma\nu_{e}\bar{\nu}_{e}$

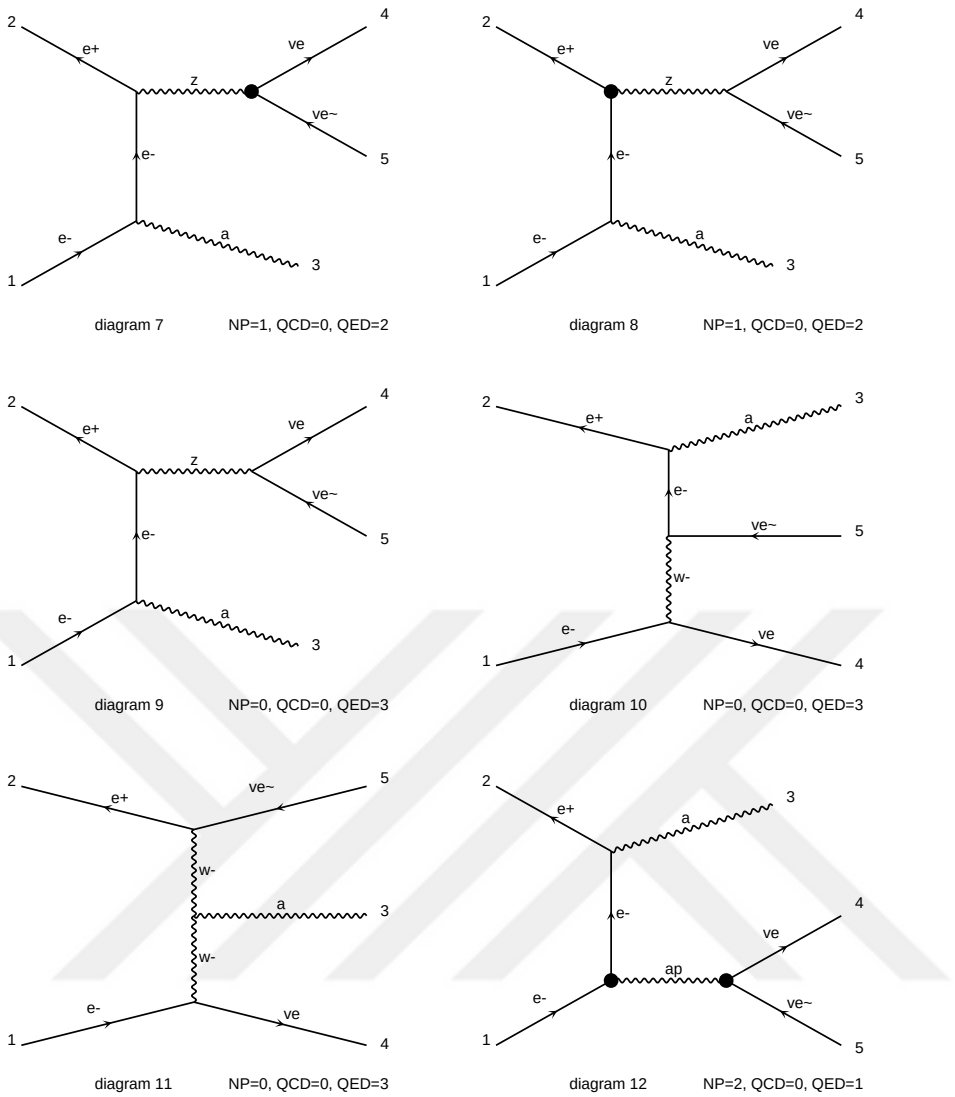


Figure A.4: 2nd set of diagrams of the process: $e^- e^+ > \gamma \nu_e \bar{\nu}_e$

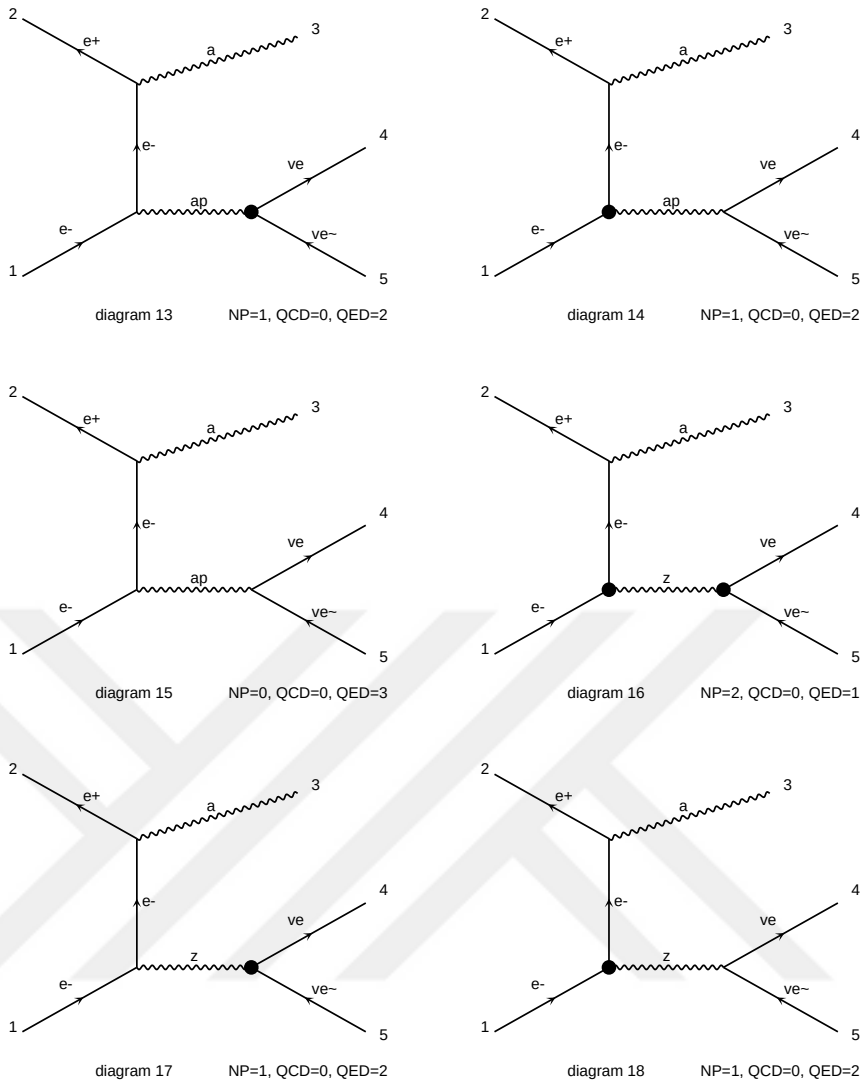


Figure A.5: 3rd set of diagrams of the process: $e^- e^+ > \gamma \nu_e \bar{\nu}_e$

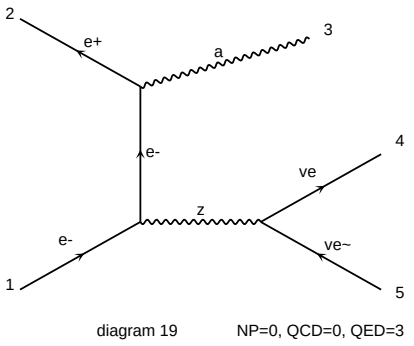


Figure A.6: 4th set of diagrams of the process: $e^- e^+ > \gamma \nu_e \bar{\nu}_e$

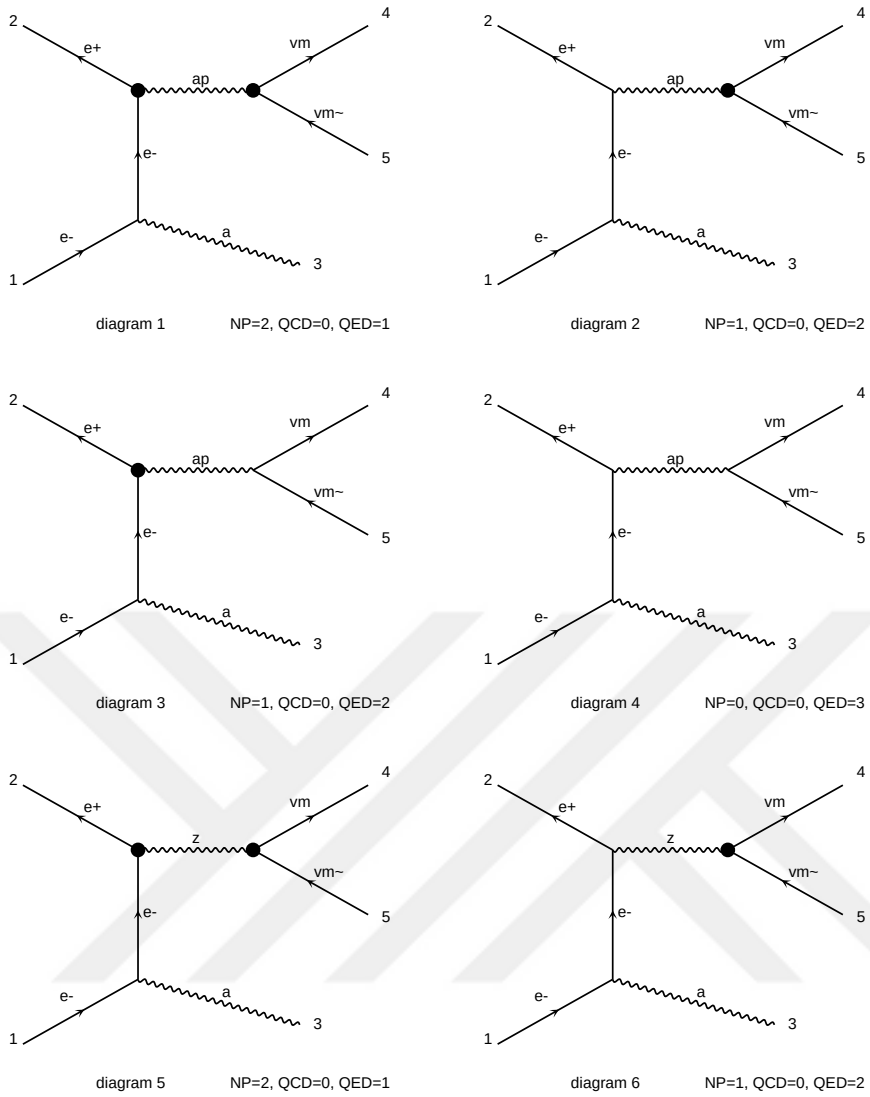


Figure A.7: 1st set of diagrams of the process: $e^- e^+ > \gamma \nu_\mu \bar{\nu}_\mu$

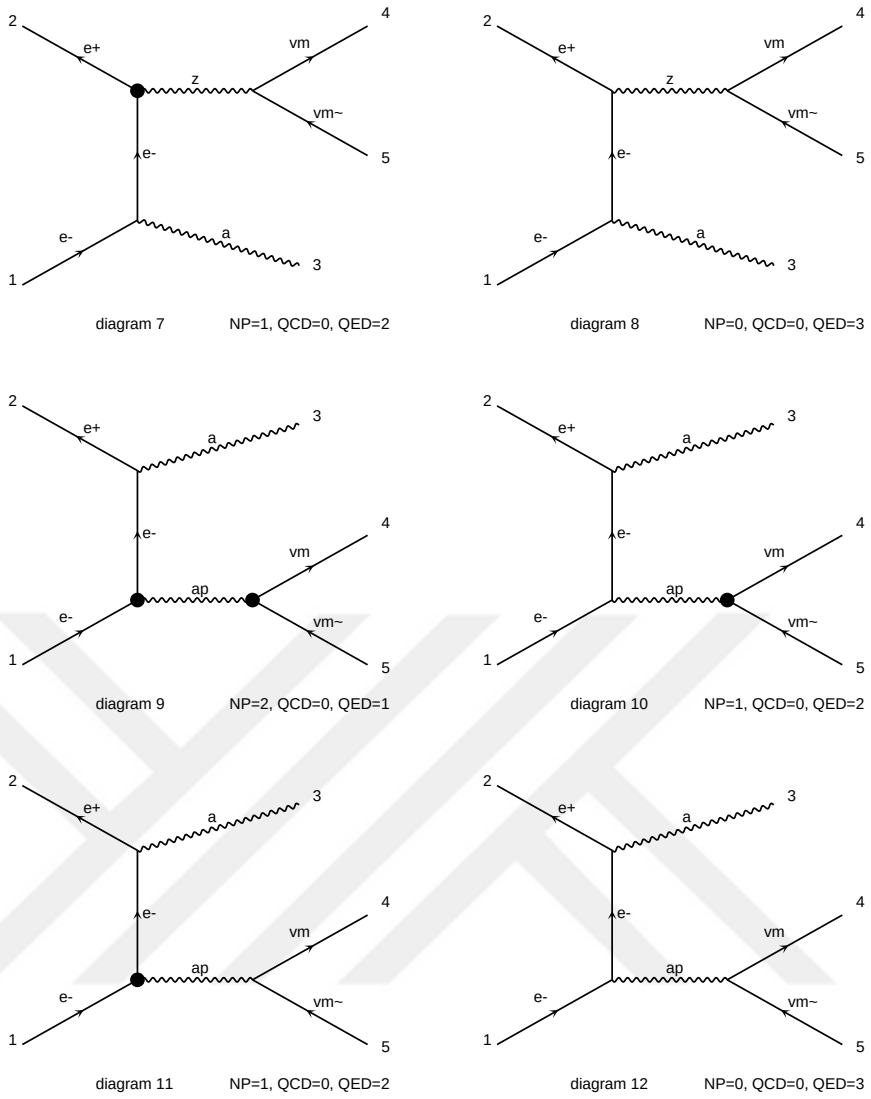


Figure A.8: 2nd set of diagrams of the process: $e^- e^+ > \gamma \nu_\mu \bar{\nu}_\mu$

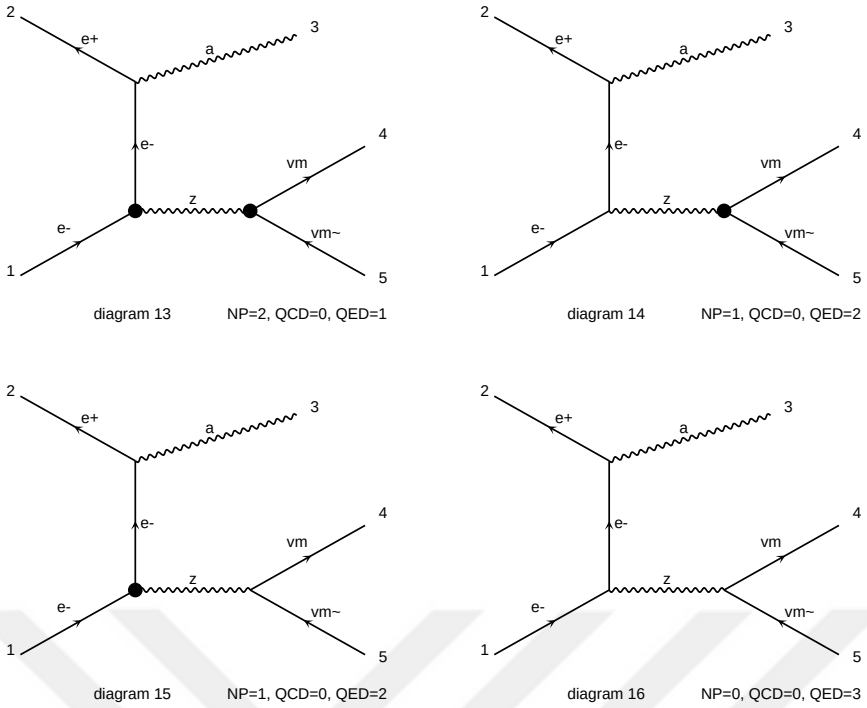


Figure A.9: 3rd set of diagrams of the process: $e^- e^+ > \gamma \nu_\mu \bar{\nu}_\mu$

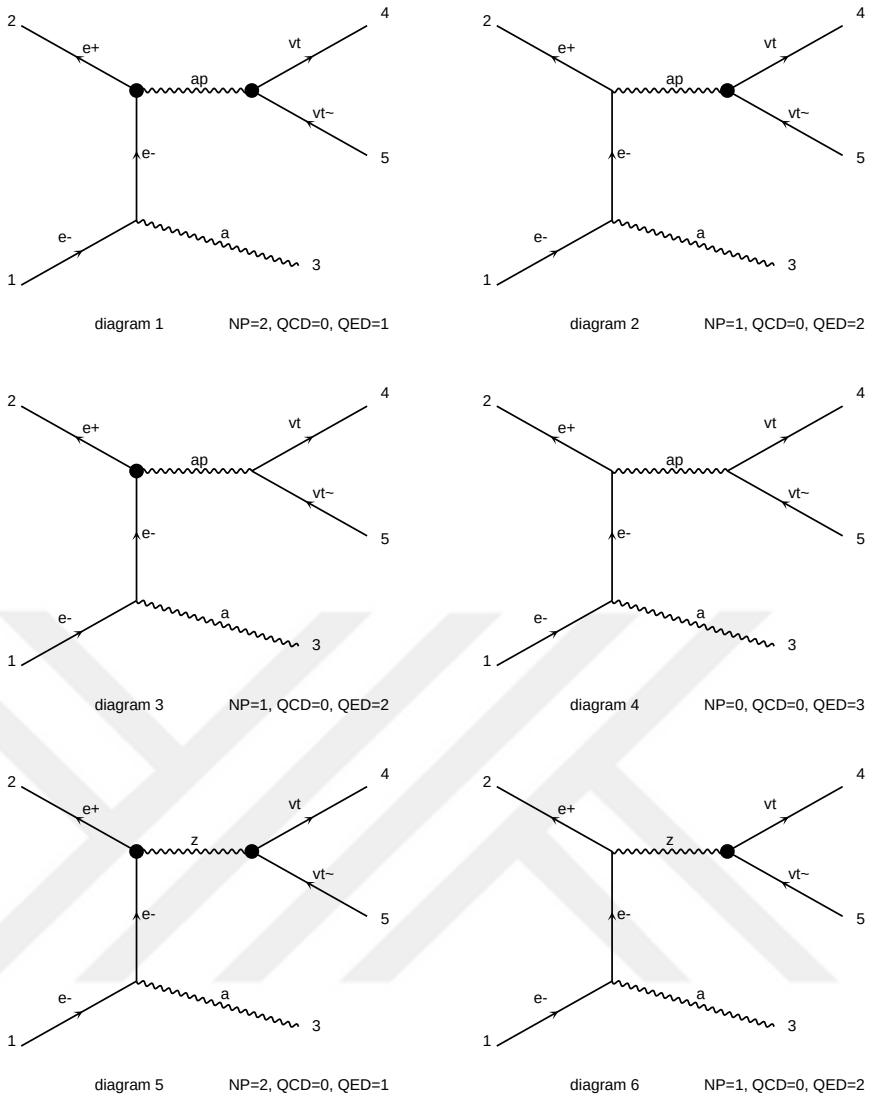


Figure A.10: 1st set of diagrams of the process: $e^- e^+ > \gamma \nu_\tau \bar{\nu}_\tau$

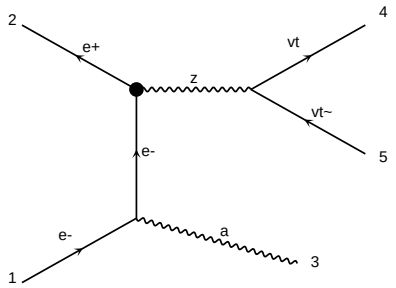


diagram 7 NP=1, QCD=0, QED=2

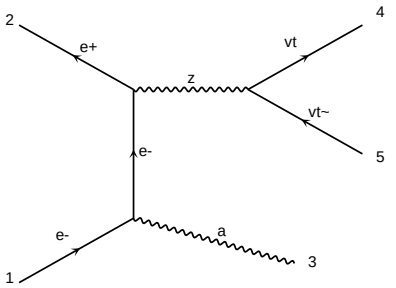


diagram 8 NP=0, QCD=0, QED=3

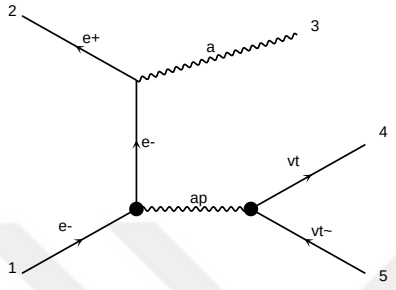


diagram 9 NP=2, QCD=0, QED=1

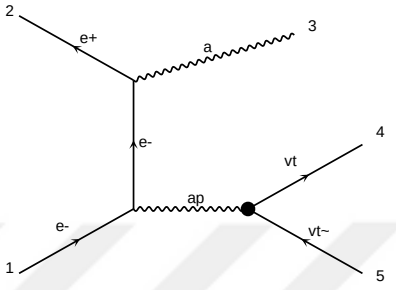


diagram 10 NP=1, QCD=0, QED=2

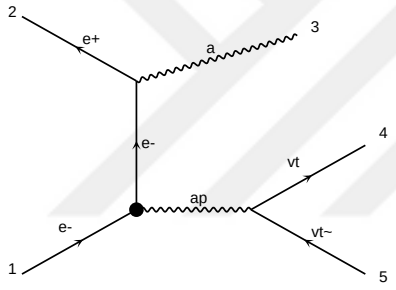


diagram 11 NP=1, QCD=0, QED=2

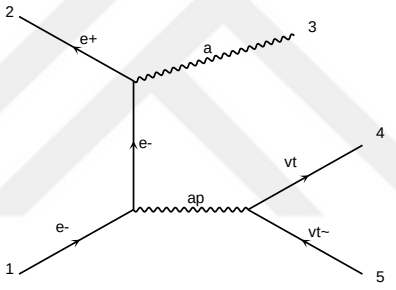


diagram 12 NP=0, QCD=0, QED=3

Figure A.11: 2nd set of diagrams of the process: $e^- e^+ > \gamma \nu_\tau \bar{\nu}_\tau$

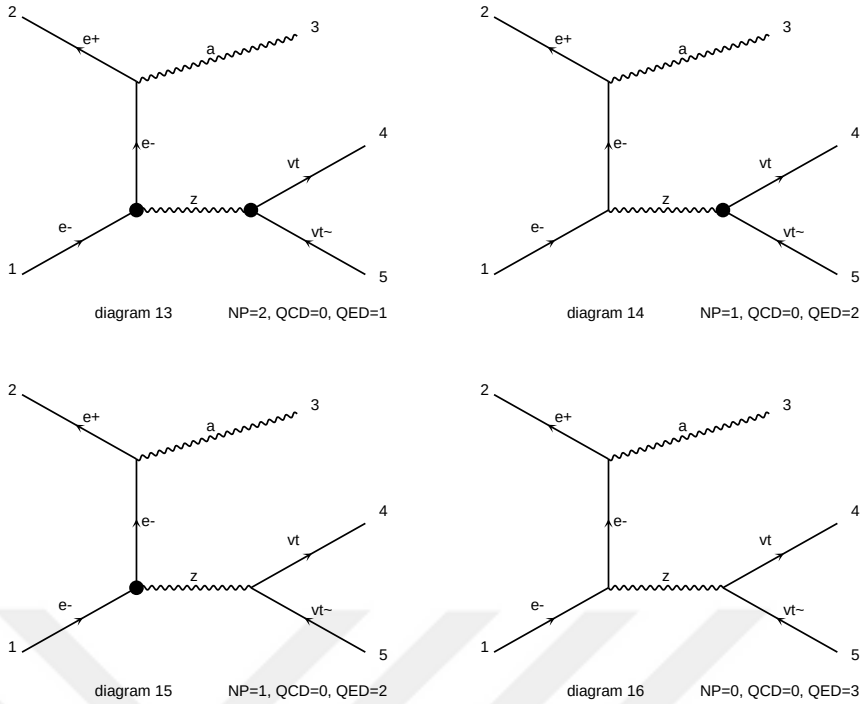


Figure A.12: 3rd set of diagrams of the process: $e^- e^+ > \gamma \nu_\tau \bar{\nu}_\tau$

A.3 Feynman Diagrams with Hidden Sector Contribution (DM Involved)

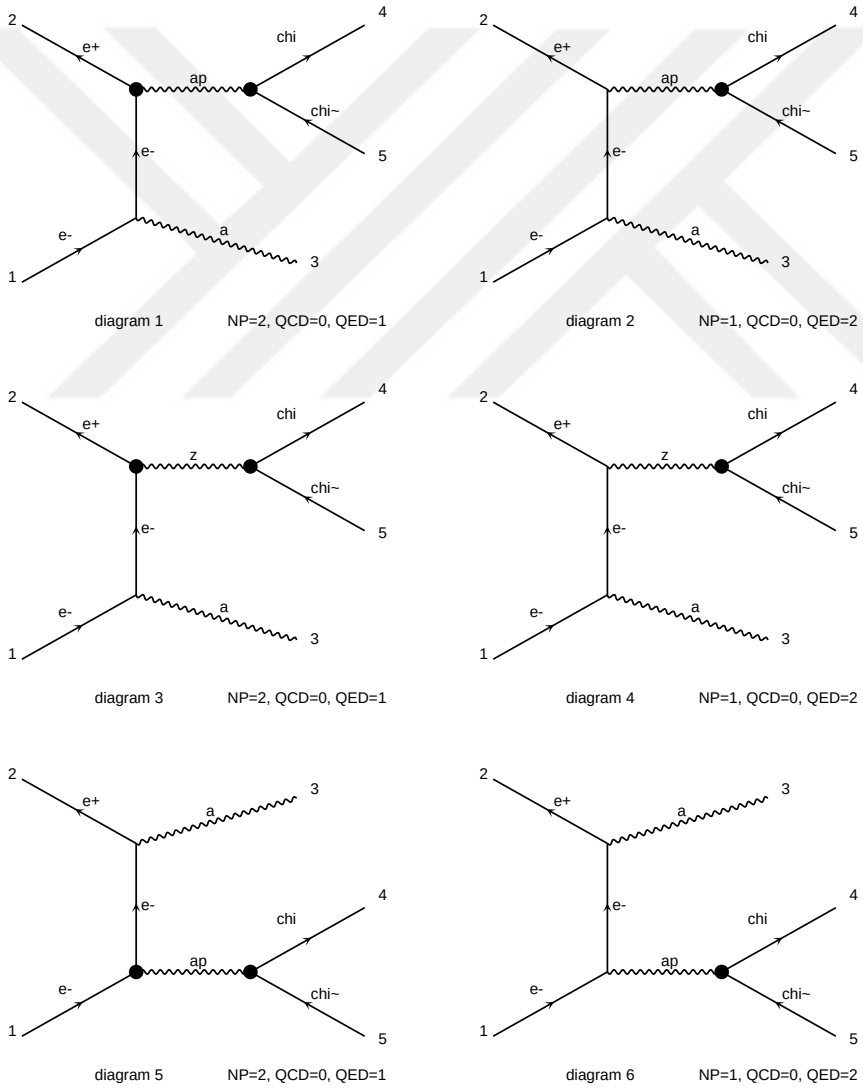


Figure A.13: 1st set of diagrams of the process: $e^- e^+ > \gamma \chi \bar{\chi}$

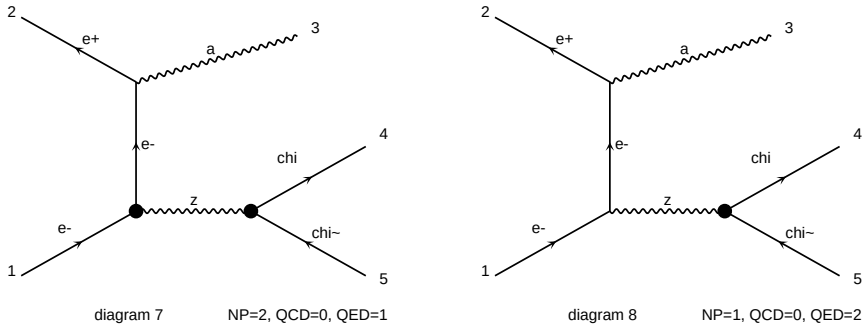


Figure A.14: 2nd set of diagrams of the process: $e^- e^+ > \gamma \chi \bar{\chi}$